Molecular Pharmacology Fast Forward. Published on August 31, 2004 as doi:10.1124/mol.104.001347

MOL # 1347

Critical Role of Reactive Oxygen Species and Mitochondrial Membrane Potential in Korean Mistletoe Lectin-induced Apoptosis in Human Hepatocarcinoma Cells

Won-Ho Kim, Won Bong Park, Bin Gao, and Myeong Ho Jung

W.H.K., M. H. J.: Division of Metabolic Disease, Department of Biomedical Science, National Institutes of Health, #5 Nokbun-dong, Eunpyung-gu, Seoul 122-701, South Korea; W. B. P.: College of Natural Sciences, Seoul Women's University, Seoul 139-774, Korea; B. G.: Section on Liver Biology, Laboratory of Physiologic Studies, National Institute on Alcohol Abuse and Alcoholism, National Institutes of Health, Bethesda, MD 20892

This work was supported by research grants from the Korean National Institutes of Health intramural research grant (347-6111-211-207).

Molecular Pharmacology Fast Forward. Published on August 31, 2004 as DOI: 10.1124/mol.104.001347
This article has not been copyedited and formatted. The final version may differ from this version.

MOL # 1347

Running title: The role of ROS and ΔΨm in VCA-induced apoptosis in hepatic cells

Corresponding author: Dr. Myeong Ho Jung, Division of Metabolic Disease, Department of Biomedical Science, National Institutes of Health, #5 Nokbun-dong, Eunpyung-gu, Seoul 122-701, South Korea. Tel: +82-2-380-1530; Fax: +82-2-354-1057; Email: jung0603@nih.go.kr

The number of Text pages: 44

The number of figures: 11

The number of references: 40

The numbers of words

Abstract: 246

Introduction: 660

Discussion: 1499

Abbreviations: VCA, *Viscum album L. coloratum* agglutinin; ROS, Reactive oxygen species; ΔΨm, mitochondrial membrane potential; NAC, N-acetyl-L-cysteine; MTP, mitochondria transition permeability; TMRM, tetramethylrhodamine methyl ester; PARP, poly (ADP-ribose) polymerase; MTT, 3-[4,5-dimethylthiazol-2-yl]-2,5-diphenyl tetrazolium bromide; DCFH-DA, dichlorodihydrofluorescein diacetate; PMSF, phenylmethylsulfonyl fluoride; TUNEL, Terminal Deoxynucleotidyl Transferase-mediated dUTP Nick-end Labeling; FACS, fluorescent-activated cell sorter; MAPK, mitogen-activated protein kinase; JNK/SAPK; c-jun NH2-terminal kinase/stress-activated protein kinase.

Molecular Pharmacology Fast Forward. Published on August 31, 2004 as DOI: 10.1124/mol.104.001347
This article has not been copyedited and formatted. The final version may differ from this version.

ABSTRACT

Viscum album L. coloratum agglutinin (VCA), isolated from Korean mistletoe, is a strong inducer of apoptosis in a variety of tumor cells; however, the underlying molecular mechanisms responsible are not clear. Here, we show that VCA induces apoptotic killing, as demonstrated by DNA fragmentation, Hoechst 33258 staining, TUNEL assay, and flow cytometry analysis in hepatocarcinoma Hep3B cells. VCA treatment results in a significant increase in reactive oxygen species (ROS) and loss of mitochondrial membrane potential ($\Delta\Psi m$). Furthermore, treatment with the antioxidant N-acetyl-L-cysteine (NAC) reduces ROS induction by VCA, preventing apoptosis in Hep3B cells, indicating that oxidative-stress is involved in VCA-mediated cell death. Our results also show rapid changes in mitochondrial transition permeability (MTP), Bax translocation, cytochrome c release, caspase-3 activity, and PARP degradation in Hep3B cells occurring in VCA-induced apoptosis. There is much evidence that implicates JNK activation with apoptosis in a variety of cellular and animal models. In this study, we show that VCA induces JNK phosphorylation, which is abolished with pretreatment with a JNK inhibitor. Moreover, Hep3B cells overexpressing JNK1 or SEK1 appear to be more susceptible to cell death from ROS and loss of $\Delta\Psi m$ induced by VCA, whereas expression of dominant-negative JNK1 or SEK1 in Hep3B cells do not. These data suggest that JNK phosphorylation may be a major regulator involved in VCA-induced apoptosis. Collectively, these results suggest that VCA induces apoptosis by inducing ROS production and a loss of $\Delta\Psi m$, in which JNK phosphorylation plays a critical role in these events.

Molecular Pharmacology Fast Forward. Published on August 31, 2004 as DOI: 10.1124/mol.104.001347
This article has not been copyedited and formatted. The final version may differ from this version.

INTRODUCTION

Extracts of mistletoe (*Viscum album L*) are therapeutically active ingredients in anti-cancer treatments (Bloksman et al., 1979; Büssing et al., 1996). The European mistletoe lectins (*Viscum album L*, VAAs), composed of A- and B-chains, have molecular weights between 55 and 63 kDa, and bind either to D-galactose alone or with N-acetyl-galactosamine (Franz, 1986; Dietrich et al., 1992). In cell culture and in animal models, VAA elicits cellular responses supporting the adjuvant effects of mistletoe extracts in cancer therapy. VAA-1 is a potent inducer of apoptosis in several tumor cell lines, inhibiting de novo protein synthesis and activating caspases (Bantel et al., 1999; Savoie et al., 2000). Additionally, VAA-1 has been shown to possess immunomodulatory activity *in vivo*, increasing levels of various cytokines, including interleukin-1, interleukin-6, and TNF-α (Hajto et al., 1998a and 1998b), to induce tumor cell death through NK cell activation.

Isolated from the Korean mistletoe (*Viscum album L. coloratum*), Viscum album L. agglutinin (VCA) is a D-galactose- and N-acetyl-galactosamine-specific lectin, which has demonstrated anticancer activity as well (Park et al., 1998; Park et al., 2000). The N-terminal amino acid and gene sequences of VCA differ from the VAA sequences (Khwaja et al., 1980), but the anticancer effect of VCA is believed to act similarly: the 34 kDa B-chain binds and anchors itself to the tumor cell surface, while the 31 kDa A-chain inhibits protein synthesis (Lyu et al., 2001; Büssing et al., 1999). However, recent studies report that liquid extracts of Korean mistletoe inhibit tumor metastasis caused by hematogenous and nonhematogenous tumor cells by suppressing tumor growth (Yoon et al., 1995) and

inhibiting tumor-induced angiogenesis (Park et al., 2001). In addition, our previous studies have demonstrated that p53 regulation is associated with telomerase inhibition in VCA-induced apoptosis (Lyu et al., 2002). Despite the known biological and physiological functions of Korean mistletoe, the exact role and molecular mechanisms involved in VCA activity, specifically the apoptotic cytotoxicity of tumor cells, as an anticancer substance are still unclear.

In many hepatocellular models of apoptosis, oxidative stress induced by reactive oxygen species (ROS) is a frequent mediator of apoptosis (Lemasters, 1999). The ability of ROS-mediated oxidative stress during massive cellular damage has been associated with lipid peroxidation, mitochondrial release of the proapoptotic proteins AIF and Cytochrome C, loss of mitochondrial membrane potential ($\Delta\Psi m$), and depletion of cellular antioxidants such as glutathione (Leist et al., 1997; Crompton, 1999). Additionally, the Jun-N-terminal kinase/stress activated protein kinase (JNK/SAPK) subfamily of mitogen activated protein kinases (MAPKs) is associated with stress responses and can mediate cellular growth and differentiation, as well as apoptosis (Gupta et al., 1995; Kyriakis et al., 1994). Recent studies have pointed toward the activation of JNK/SAPK as the signal transducer for oxidative stress, growth factor deprivation, and cytokine release in several tumor cell lines (Xia et al., 1995). The proapoptotic effects of JNK include induction of cytochrome c release from mitochondria through phosphorylation of Bcl-2 and Bcl-xL, as well as activation of FasL, TNF-α, c-myc, and p53 promoters.

It has been reported that VAA-1 alters mitochondrial transmembrane potential and

increases intracellular levels of ROS in human neutrophils, and induces apoptosis through ROS-independent and Mcl-1-dependent mechanisms (Lavastre et al., 2002). However, earlier studies have reported that Korean mistletoe lectin- and European mistletoe-induced apoptosis were regulated by JNK/SAPK activation and caspase-3 and -7 activation in human leukemia cells (Savoie et al 2000; Park et al., 2000). Although it has been demonstrated that mistletoe lectins induce apoptosis through several apoptotic-related mechanisms, the relationships between release of mitochondrial proteins, caspase activation, ROS production, and loss of MPT, remain unclear. Therefore, the possibility that VCA induces apoptosis through mitochondrial damage by ROS-dependent mechanisms in Hep3B cells has not been excluded.

In this study, intracellular ROS formation and loss of $\Delta\Psi m$ were observed to play important roles in mediating apoptotic processes induced by VCA. These processes may be regulated by activation of the SEK/JNK pathway. These studies provide a rational basis for new clinical perspectives in future mistletoe therapy.

Molecular Pharmacology Fast Forward. Published on August 31, 2004 as DOI: 10.1124/mol.104.001347
This article has not been copyedited and formatted. The final version may differ from this version.

MATERIALS AND METHODS

Materials. Anti-ERK1/2, anti-phospho-ERK1/2, anti-p38, anti-phospho-p38, anti-JNK, and anti-phospho-JNK antibodies were obtained from Cell Signaling Technology (Beverly, MA). Anti-PARP, anti-Bcl-2, anti-Bax, anti-Bad, and anti-Bcl-XL antibodies were obtained from BD Pharmingen (San Diego, CA). Anti-cytochrome c antibody, anti-GCK, and anti-VDAC were purchased from Santa Cruz Biotechnology Inc. (Santa Cruz, CA). GST-c-Jun was purchased from Cell Signaling Technology (Beverly, MA). Dichlorodihydrofluorescein diacetate (DCFH-DA), DiOC6, tetramethylrhodamine methyl ester perchlorate (TMRM), Alexa-488 anti-rabbit IgG, and MitoTracker Red CMXRos were purchased from Molecular Probes (Eugene, OR). SP600125 and the caspase-3 inhibitor I (DEVD-CHO) was purchased from Calbiochem (San Diego, CA). N-acetylcysteine (NAC), cyclosporin A (CsA), phenylmethylsulfonyl fluoride (PMSF), aprotinin, leupeptin, penicillin, streptomycin, rhodamine 123 (Rh123), mouse monoclonal anti-human β-actin (Clone AC-15), propidium iodide (PI), and other common chemicals all came from Sigma (St. Louis, MO). The plasmids pcDNA3-HA-JNK1 wild type (wt), pEBG-SEK1 wt, and its dominant negative mutant pcDNA-HA-JNK1-KR (Lys-Arg), or pEBG-SEK1-KR was from Dr. B. J. Song (National Institute of Alcohol abuse and Alcoholism, NIH, Bethesda, MD), which have been described in previous papers (Soh et al., 2000).

Preparation of VCA, mistletoe extract or powder of mistletoe. Korean mistletoe (*Viscum album* L. var. *coloratum*) grown on oak trees were collected in the winter in South Korea. Leaves, berries, and 1- to 4-year old plants stems were sorted and chopped

Molecular Pharmacology Fast Forward. Published on August 31, 2004 as DOI: 10.1124/mol.104.001347
This article has not been copyedited and formatted. The final version may differ from this version.

into slices. Crude protein solutions were prepared by binding the protein onto the cation exchanger as was described previously (Na et al., 1996; Park et al., 2000). Briefly, 3.5 g of SP Sephadex C-50 (Pharmacia, Uppsala, Sweden) was added to 1 L of aqueous extract and stirred at 4ºC. The gel filled chromatography column was washed with 0.1 M acetate buffer (pH 4.0), and the proteins were eluted with buffer solution (0.1 M Tris-HCl, pH 8.0, 0.5 M NaCl). The solution was put on the column filled with asialofetuin-Sepharose 4B, and the column was washed with PBS and concentrated by ultrafiltration (MW= 10 kDa, Amicon Corp, Danvers, MA, USA). Purity and molecular mass were determined by SDS-PAGE as described previously (Büssing et al., 1999; Park et al., 2001). The hemagglutination and sugar specificity of lectin was measured as described previously (Park et al., 1998). To prepare mistletoe extract, the leaves, berries and 1- to 4-year old stems of the plants sorted and chopped in slices and then crushed with 10 volumes of saline between two rollers going in opposite directions in a vegetable juice miller (Angel life Co., Korea). The mixture was separated by filtration through a cheesecloth, and centrifuged at 12,000 rpm for 30 min. Thereafter, the supernatant was filtered in stages with 60, 20, 7.2, and 0.45 μm pore sizes and lyophilized. To prepare powder of mistletoe, the leaves, berries, and 1- to 4-year old plant stems were lyophilized and ground into powder.

Cell Culture and Determination of Cell Viability. Monolayers of Hep3B cells were maintained in culture at 37ºC and 5% CO_2 in DMEM supplemented with 10% (v/v) fetal bovine serum (FBS), 100 IU/ml penicillin, and 100 μg/ml streptomycin. Hep3B cells grown for 1 day in 96-well microtiter plates (1 X 10^4/well) were incubated with varying

Molecular Pharmacology Fast Forward. Published on August 31, 2004 as DOI: 10.1124/mol.104.001347
This article has not been copyedited and formatted. The final version may differ from this version.

concentrations of VCA for different times. Cell viability was measured using MTT (3-[4, 5-dimethylthiazol-2-yl]-2, 5-diphenyl tetrazolium bromide) as a substrate.

Stable Transfection. Hep3B cells were grown in 6-well culture plates to about 50-60% confluence. Wild-type JNK1 and SEK1 or dominant-negative JNK1 (Lys→Arg) and SEK1 (Lys→Arg), and vector control DNA were transfected into Hep3B cells using a lipofectin reagent (GIBCO, Gaithersburg, MD). After 16 h, the medium was replaced with normal growth medium and cells were grown for an additional 48 h. Then the cells were exposed to a selective concentration (as determined by 'a killing curve') of 400 μg/ml of geneticin (G418-sulfate, GIBCO) to isolate stably transfected cells. Positive colonies were passed 3 times before selecting unique clones. The stably transfected cell lines were maintained under constant selective pressure in the continued presence of 400 μg/mL of geneticin. After transfection with the respective cDNA, the level of protein expressed was determined by western blotting using the specific antibody toward each target protein.

Western Blotting. Cells were lysed in RIPA buffer (50 mM Tris, pH 7.5, 1% Nonidet P-40, 150 mM sodium deoxycholate, 150 mM NaCl, 1 mM EDTA, 1 mM sodium orthovanadate, 1 mM sodium fluoride, 1 mM phenylmethylsulfonyl fluoride, 1 μg/ml aprotinin, 1 μg/ml leupeptin, and 1 μg/ml pepstatin), and then vortexed and centrifuged at 16,000 rpm at 4°C for 10 min. The supernatants were mixed in Laemmli loading buffer, boiled for 4 min, and then subjected to SDS-PAGE. After electrophoresis, proteins were transferred onto nitrocellulose membranes and blotted against primary antibodies for 16 h. Membranes were washed with TPBS (0.05% [vol/vol] Tween 20 in phosphate buffered

Molecular Pharmacology Fast Forward. Published on August 31, 2004 as DOI: 10.1124/mol.104.001347
This article has not been copyedited and formatted. The final version may differ from this version.

saline (PBS) [pH 7.4]) and incubated with a 1:4000 dilution of horseradish peroxidase-conjugated secondary antibodies for 45 min. Protein bands were visualized by an enhanced chemiluminescence reaction (Amersham Pharmacia Biotech, Piscataway, NJ).

Terminal Deoxynucleotidyl Transferase-mediated dUTP Nick-end Labeling (TUNEL*).* Apoptotic cells were detected using Apop Tag (Oncor, Gaitherburg, MD), an *in situ* apoptosis detection kit. Briefly, cells were fixed on slides and then incubated with terminal transferase and avidine-labelled-dUTP, followed by further incubation with FITC-labeled anti-avidine antibody. The slides were then examined under fluorescence microscopy.

Flow Cytometric Analysis of Apoptosis. After trypsinization, approximately 10^6 cells were collected by centrifugation at 1,000g for 5 minutes. Cells were then washed in PBS followed by resuspension and fixation in 70% ethanol for approximately 2 h. Next, cells were washed with PBS and resuspended in 500 µL PBS containing 100 µg/mL RNase, followed by a 30-min incubation period at room temperature. Cellular DNA was then stained by the addition of 50 µg/mL PI, and cells were analyzed on a FACScan using Cellquest software (Becton Dickinson).

DNA Fragmentation. Cultured hepatocytes were washed twice with PBS and lysed in buffer (100 mM NaCl, 10 mM Tris-HCl, pH 8.0, 25 mM EDTA, 0.5% SDS, and 0.1 mg/ml proteinase K) at 37ºC for 18 h. DNA was extracted with an equal volume of phenol/chloroform (1:1) and precipitated at –70ºC. DNA pellets were resuspended in 10 µl of 10 mM Tris (pH 7.8), 1 mM EDTA buffer and incubated for 1 h at 37ºC with 1 µg/ml RNase (Roche Molecular Biochemicals) to remove RNA. DNA pellets were

Molecular Pharmacology Fast Forward. Published on August 31, 2004 as DOI: 10.1124/mol.104.001347
This article has not been copyedited and formatted. The final version may differ from this version.

electrophoresed for 2-3 h at 90 V on 1.8% agarose gels. The gel was stained with ethidium bromide and the DNA fragments were visualized under ultraviolet light.

Immunocytochemistry. Hep3B cells were grown on poly-D-lysine-coated coverslips in 6-well plates. Cells were pretreated with 100 nM MitoTracker CMXRos during the last 30 minutes of treatment, washed with PBS, and fixed with 3.7 % formaldehyde in PBS for 10 min at room temperature. The coverslips were soaked in a blocking solution (PBS containing 5 % bovine serum albuminand 0.2 % Triton X-100) for 30 min and incubated with anti-Bax antibody (1:300) overnight at 4°C and then with Alexa-488 anti-rabbit IgG antibody (1: 400) for 30 min in the blocking solution before mounting. The fluorescence was analyzed by confocal microscope (NIKON). The cells exhibiting strong punctuate staining of Bax, which overlapped with the distribution of MitoTracker CMXRos, were counted as cells with mitochondrially localized Bax.

Measurement of ROS. Intracellular ROS generation was monitored by flow cytometry, using fluorescence produced from 2', 7'-dichlorofluorescein (DCF) after being oxidized from dichlorodihydrofluorescein diacetate (DCFH-DA) (Lavastre et al., 2002) (Molecular Probes, Eugene, OR). In brief, after treatment with 10 ng/mL VCA, cells were incubated with 5 uM DCFH-DA during the last 30 min at 37ºC and then detached with trypsin. Cells were washed twice with PBS and resuspended with PBS containing 1% FBS. Fluorescence intensity was measured using a FACSCalibar flow cytometer (Becton Dickinson).

Measurement of Mitochondrial Membrane potential ($\Delta\Psi m$). To measure mitochondrial membrane potential ($\Delta\Psi m$), cells were incubated with $DiOC_6$ (100 nM,

Molecular Pharmacology Fast Forward. Published on August 31, 2004 as DOI: 10.1124/mol.104.001347
This article has not been copyedited and formatted. The final version may differ from this version.

Molecular Probes Inc.) during the last 30 min of treatment (Pastorino et al., 2001). $DiOC_6$ is a fluorescent dye that is incorporated into mitochondria in a $\Delta\Psi m$-dependent manner. Accumulation of a membrane-permeable cationic fluorescent dye, Rh123 (Sigma), was used to further confirm $\Delta\Psi m$ (Bai et al., 1999). Cells were incubated with 5 μg/ml Rh123 for 40 minutes prior to treatment end. Cells were then harvested by trypsinization, washed with 1 X PBS, and resuspended in PBS (for $DiOC_6$) and PBS containing 25 μg/ml PI (for Rh 123). Fluorescence intensity was determined by flow cytometry.

Analysis of mitochondrial permeability transition (MPT) using laser scanning confocal microscope. To monitor MPT changes, the fluorescent probe TMRM (red fluorescence) was used as described by Pastorino and Hoek (Pastorino et al., 2001). TMRM is a cationic fluorophore that accumulates electrophoretically in normal mitochondria because of the negative $\Delta\Psi m$. Decreases in TMRM red fluorescence in mitochondria indicates disruption of $\Delta\Psi m$. Briefly, Hep3B cells were cultured in 4-well chamber slides. After washing with PBS, cells were first loaded with 0.5 mM TMRM in FBS-free culture medium at 37ºC for 15 min. After staining, cells were washed twice with PBS and then mounted onto a laser scanning confocal microscope (Zeiss LSM 410) and incubated in FBS-free medium for treatment with VCA (10 ng/ml). The red fluorescence of TMRM was excited simultaneously with 568 nm lines from an argon-krypton laser.

Isolation of Cytosol and Mitochondrial Fractions. Cells were plated on 10 cm^2 petri dishes at a density of 5 X 10^6 cells/dish. Following treatment, cells were harvested by trypsinization, washed once in PBS, and resuspended in 3 volumes of isolation buffer (20

Molecular Pharmacology Fast Forward. Published on August 31, 2004 as DOI: 10.1124/mol.104.001347
This article has not been copyedited and formatted. The final version may differ from this version.

μM/ml Hepes, pH 7.4, 10 μM/ml KCl, 1.5 μM/ml $MgCl_2$, 1 μM/ml sodium EDTA, 1 μM/ml DTT, 10 μM/ml PMSF, 10 μg/ml leupeptin, and 10 μg/ml aprotinin in 250 μM/ml sucrose). After chilling on ice for 5 minutes, the cells were disrupted by 50 strokes in a glass homogenizer. The homogenate was centrifuged twice at 2,500 g at 4°C to remove unbroken cells and nuclei. Then the mitochondria were pelleted by centrifugation at 9,000 g at 4°C for 30 minutes to obtain the heavy membrane (HM) fraction enriched with mitochondria. The supernatant from the initial 9,000 g centrifugation was centrifuged again at 100,000 g to give cytosolic supernatant and light membrane (LM) fractions. Mitochondrial and cytosolic fractions (60 μg) were separated on 15% SDS-PAGE gels and immunoblotted with antibody against cytochrome c.

Bax oligomerization assay. The Bax oligomerization assay was adapted as described previously (Majewski et al., 2004). Briefly, the mitochondria-enriched fraction from isolated cells were subjected to protein cross-linking by incubation in freshly prepared 10 mM bismaleimidohexane (Pierce)-16.8% dimethyl sulfoxide-PBS for 30 min at room temperature with occasional mixing. Samples were boiled for 5 min in 1 X laemmli buffer, resolved by SDS-PAGE (12 %), transferred onto nitrocellulose membranes , and subjected to Western blot analysis using an anti-Bax antibody. For Bax-VDAC binding assay, total cellular extracts were immunoprecipitated with anti-VDAC antibody, then washed twice with lysis buffer, and then subjected to Western blot against anti-Bax antibody.

JNK kinase To assess JNK activity, cells were washed twice with PBS (pH 7.4) containing 1 mM sodium vanadate, and lysed in 0.5 ml of lysis buffer (30 mM Tris, pH

Molecular Pharmacology Fast Forward. Published on August 31, 2004 as DOI: 10.1124/mol.104.001347
This article has not been copyedited and formatted. The final version may differ from this version.

7.5, 150 mM sodium chloride, 1 mM phenylmethylsulfonyl fluoride, 1 mM sodium orthovanadate, 1% Nonidet P-40, 10% glycerol). Total cellular extracts were immunoprecipitated with anti-JNK antibody overnight, then washed twice with lysis buffer, and then once with kinase buffer (50 mM Tris pH 7.4, 5 mM $MgCl_2$, 10 mM $MnCl_2$, 0.1 mM sodium orthovandate). Pellets were resuspended in 50 ml of kinase buffer containing 2 μg of GST-c-Jun (Cell Signaling Technology, Beverly, MA) and 5 mCi of [γ-^{32}P] ATP, and incubated at 30°C for 10 min. The reaction samples were boiled in SDS sample buffer containing 2.5% 2-mercaptoethanol for 5 min. The solubilized proteins were resolved by SDS-PAGE and quantified by phosphorimaging.

Enzymatic Assay of Caspase-3. Cleavage of the caspase-3 substrate I (Ac-DEVD-*p*NA) (Calbiochem, San Diego, CA) was used as a measure of caspase-3 activity. The *p*-Nitroaniline was used as the standard. Cleavage of the substrate was monitored at 405 nm and the specific activity was expressed in pmol of the product (nitroaniline) per minute per mg protein.

Statistical Analysis. For comparing values obtained in 3 or more groups, one-factor analysis of variance was used, followed by Turkey's post hoc test, and $P<0.05$ was taken to imply statistical significance.

Molecular Pharmacology Fast Forward. Published on August 31, 2004 as DOI: 10.1124/mol.104.001347
This article has not been copyedited and formatted. The final version may differ from this version.

RESULTS

VCA induces apoptosis in hepatocytes. First, to examine the cytotoxic effect of VCA on a human hepatocellular carcinoma cell line, Hep3B cells were treated with VCA at different times and doses. Cell viability was measured by the MTT assay or by trypan blue exclusion. VCA significantly inhibited cell viability in a time- and dose-dependent manner (Fig. 1A). To investigate whether VCA-induced cell death was due to apoptosis, DNA fragmentation was assessed. While no evidence of genomic DNA cleavage was detected in control cells, VCA-treated cells were markedly fragmented at nucleosomal intervals, ~ 200 bp, in a time- and dose-dependent manner (Fig. 1B). For further confirmation, the cells were also treated with 10 ng/mL of VCA for 12h and morphological changes were observed under a fluorescent microscope after Hoechst 33258 staining. Compared to untreated controls, VCA-treated cells exhibited a number of morphological changes characteristic of programmed cell death. During the apoptotic course, blebbing of the cell membrane occurred and the cells were fragmented into characteristic apoptotic bodies (Fig. 1C). Additionally, we also examined TUNEL assay and DNA content by FACS analysis. VCA treatment caused a 4.8 ± 0.5 fold increase in TUNEL-positive Hep3B cells (Fig. 1D), and flow cytometric analyses showed that treatment with VCA markedly induced apoptosis (M1, sub-G1 phase, 2.70% in non-treated Hep3B cells vs. 18.41% in VCA-treated Hep3B cells) (Fig. 1E). Taken together, these findings indicate that VCA treatment strongly induced apoptosis in Hep3B cells.

VCA induces apoptotic killing through a caspase-3-dependent mechanism in Hep3B Cells. The role of caspase-3 activation as an important mediator of apoptosis is well

established (Allen et al., 1998). Therefore, the effects of VCA on caspase-3 activation in Hep3B cells were determined. After the cells were treated with VCA for various time periods and doses, lysates were obtained to measure the catalytic activity of the caspase-3 protease. As shown in Fig. 2A, the activity of caspase-3-like proteases was significantly increased beginning 6 h after VCA treatment and reached a maximal level after 12 h (5.8-fold). VCA also significantly induced activation of caspase-3-like proteases in a dose-dependent fashion (Fig. 2B), observed first as a 4-fold increase of caspase-3-like protease activity after 12 h of treatment with 10 ng of VCA. Pretreatment of the cells with a specific caspase-3 inhibitor, z-DEVD-CHO (100 uM), significantly reduced VCA-induced caspase-3 activation (Fig 2A and B) and apoptosis (Fig. 2C). To determine whether VCA-activated caspase-3 is functionally active in these cells, cleavage of poly ADP-ribose polymerase (PARP) was examined by Western blot analysis. As shown in Fig. 2D, treatment with VCA rapidly caused cleavage of PARP in Hep3B cells; this cleavage was markedly inhibited by pretreatment with the caspase 3 inhibitor, z-DEVD-CHO.

VCA alters antiapoptotic and proapoptotic protein expression and induces Cytochrome C release from mitochondria. Since the expression levels of the proapoptotic Bax and antiapoptotic Bcl-2 proteins and their ratios are considered critical factors for initiating apoptosis through mitochondrial damage (Gross et al., 1999), the expression of several antiapoptotic and proapoptotic proteins in VCA-treated Hep3B cells was examined. As shown in Fig. 3A, the expression of Bcl-xL and Bcl-2 was reduced about 3.2-fold and 2.3-fold, respectively, whereas expression of Bax significantly increased by 2.9-fold after treatment for 24 h. In contrast to changes in Bax and Bcl-xL

Molecular Pharmacology Fast Forward. Published on August 31, 2004 as DOI: 10.1124/mol.104.001347
This article has not been copyedited and formatted. The final version may differ from this version.

protein expression, considerable changes in Bad and Apaf-1 expression was not detected. Next, we examined whether expression levels of Bcl-2-related proteins was modified by inhibition of apoptosis by caspase-3 inhibitor. Results show that changes in Bcl-2-related protein expression induced by VCA was not significantly affected by the addition of the caspase-3 inhibitor (Fig. 3B), suggesting that alterations in Bcl-2 family proteins following VCA treatment may not be a late event in apoptosis or reflect secondary apoptosis changes. Release of mitochondrial cytochrome C from cytosol into mitochondria is a key step in the mitochondrial pathway of apoptosis (Esposti et al., 1999). Therefore, we examined whether cytochrome C release was observed in VCA-treated Hep3B cells. As shown in Fig. 3C, VCA treatment caused cytochrome C release from the mitochondria into the cytosol at 6 h, continuing through 24 h. These results suggest that VCA-induced apoptosis may be regulated through mitochondrial damage.

VCA induces the translocation of Bax into mitochondria through conformational change as an early event in apoptosis. Recent studies have suggested that some apoptosis-promoting conditions induce Bax translocation into mitochondria and conformational changes in Bax (Gilmore etal., 2000; Putcha et al., 1999) that involve in releasing cytochrome C. To investigate this hypothesis, we examined whether VCA induces Bax translocation into mitochondria during apoptosis by experiments using FITC-Bax and MitoTracker-CMXRos, a mitochondrial marker. Our results show that FITC-Bax was localized mainly in the cytosol in normal Hep3B cells, but was distributed in both the cytosol and mitochondria in VCA-treated Hep3B cells (Fig 4A). The translocation of Bax into mitochondria was observed beginning 6 h after treatment of

VCA, and peaked at 12 h (Fig.4B). The addition of 100 μM caspase-3 inhibitor had little effect on Bax translocation induced by VCA (data not shown), demonstrating that VCA-induced Bax translocation may be an early event necessary for apoptosis by caspase-3. The molecular mechanism(s) underlying Bax subcellular redistribution, however, remains a matter to be determined. Previous reports have suggested that conformational changes in Bax through dimerization or direct binding to voltage-dependent anion channels (VDAC), a major permeability pathway for metabolites in the mitochondrial outer membrane, is required for mitochondria-mediated apoptosis (Wei et al., 2001). To explore this hypothesis, we examined whether VCA induces the interaction of Bax with VDAC using isolated mitochondrial fractions. As shown in figure 4C, the interaction of Bax with VDAC was significantly increased in VCA-treated cells. Additionally, oligomerization of Bax within the mitochondria is believed to play a pivotal role in the induction of cytochrome C release (Wei et al., 2001). Therefore, whether VCA induces Bax oligomerization leading to cytochrome C release from mitochondria was also examined. As shown in Figure 4D, VCA accelerated and amplified Bax oligomerization in a time-dependent manner, consistent with Bax translocation into mitochondria. These results suggest that VCA-induced apoptosis may be regulated through mitochondrial damage, including alterations in Bcl-2-related proteins and Bax conformational changes.

VCA induces ROS production and reduces mitochondrial membrane potential ($\Delta\Psi m$). Mitochondrial damage is important in cell death, and in some models of apoptosis, it is an early occurring event (Lemasters, 1999). Elevated amounts of

Molecular Pharmacology Fast Forward. Published on August 31, 2004 as DOI: 10.1124/mol.104.001347
This article has not been copyedited and formatted. The final version may differ from this version.

intracellular ROS are sufficient to trigger cell death, and it has been suggested that ROS are biochemical mediators of apoptosis (Pastorino et al., 2001). Therefore, to determine whether ROS is involved in the regulation of apoptosis induced by VCA, the fluorescent DCFH-DA product was determined using flow cytometry. As shown in Fig. 5A (left panel) and B (opened bar), VCA induced greater production of ROS in Hep3B cells than did control cells (M1 46.62% in control cells vs. 73.38% in VCA-treated Hep3B cells) (ROS peak shifted to the right). Next, we examined whether VCA induced-ROS production in hepatocytes could be coincident with changes in $\Delta\Psi m$ during apoptosis in these cells. To this end, we used the fluorescent lipophilic cation, DiOC6, as an indicator of the energy state of the mitochondria. As shown in Fig. 5A (right panel) and B(filled bar), VCA treatment led to a rapid drop in mitochondrial energy, as reflected by a decrease in fluorescence from baseline after 12 h of treatment (M1 47.55% in control cells vs. 77.43% in VCA-treated Hep3B cells) ($\Delta\Psi m$ peak shifted to the left, indicating that fewer cells retained DiOC6 in their mitochondria). Moreover, the antioxidant N-acetyl-L-cysteine (NAC) (Kowaltowski et al., 1998) suppressed ROS production and loss of $\Delta\Psi m$ induced by VCA (Fig. 5A and B), and protected cells from apoptosis (Fig. 5C). These data demonstrate that VCA-induced apoptosis may be closely related to mitochondrial function and membrane permeability. To visualize the changes in mitochondrial permeability transition (MPT) caused by VCA, cells were first loaded with TMRM and then treated with VCA in an FBS-free medium. The bright mitochondria were stained with red-fluorescing TMRM, which is typical of polarized mitochondria in Hep3B cells (Fig. 6A). After treatment with VCA for 50 minutes, the intensity of TMRM

fluorescence in Hep3B cells decreased significantly. This fluorescence decreased further after 90 min of VCA exposure, and was no longer detectable after 2 h. TMRM fluorescence was reduced to 38.4 ± 7.6% of control cells within 50 min (Fig. 6B). The loss of mitochondrial TMRM was prevented by the addition of the antioxidant NAC (Fig. 6A). Addition of NAC attenuated the decrease in mitochondrial TMRM fluorescence by 87.5% (Fig. 6B). Consistent with this inhibition, NAC also inhibits the release of cytochrome C from mitochondria into cytosol and the change of Bcl-2-related proteins induced by VCA (Fig. 6C). These results suggest that VCA-induced apoptosis is mediated in an oxidative stress-dependent manner, including ROS production, loss of $\Delta\Psi m$, and MPT change.

JNK phosphorylation plays a critical role in ROS production and loss of $\Delta\Psi m$ induced by VCA. To examine the mechanism involved in ROS production and the loss of $\Delta\Psi m$ in VCA-mediated apoptosis, we studied the possible involvement of several MAP kinases involved in early signal transduction, JNK/SAPK, ERK1/2, and p38 MAPK. This was accomplished by measuring the activities of JNK/SAPK, ERK1/2, and p38 by Western blot analysis using specific phospho-antibodies. As shown in Fig. 7A, as early as 10 min after VCA treatment, JNK phosphorylation was strongly induced, and persisted for up to 30 min. In contrast, neither ERK1/2 nor p38 was strongly activated following VCA treatment. Expression of these proteins was confirmed using antibodies against JNK, ERK, and p38 MAPK. To further confirm induction of JNK activity by VCA, we used an immunocomplex kinase assay using GST-c-jun as a substrate to measure JNK/SAPK activity. As shown in Fig. 7B, VCA treatment rapidly induced JNK activation with peak

Molecular Pharmacology Fast Forward. Published on August 31, 2004 as DOI: 10.1124/mol.104.001347
This article has not been copyedited and formatted. The final version may differ from this version.

effect occurring at 20 min and returning to basal levels at 60 min, while expression of JNK protein remained unchanged. Consistent with JNK activation, VCA also activated SEK, directly upstream of JNK, at 10 min and remained activated for 20 min. These data suggest that JNK phosphorylation may be a major regulator involved in the induction of ROS production and loss of $\Delta\Psi m$ during VCA-induced apoptosis.

To determine this possibility, we studied the effects of the JNK inhibitor, SP600125, on apoptosis, ROS production, and loss of $\Delta\Psi m$. As shown in Fig. 8A, pretreatment with 30 uM SP600125 markedly inhibited JNK activation induced by VCA. From the results of DNA fragmentation and DNA content analysis, SP600125 pretreatment significantly inhibited the rate of VCA-induced apoptosis (Fig 8B and C). Consistent with this inhibition, the levels of VCA-induced ROS production and loss of $\Delta\Psi m$ were also significantly decreased from pretreatment with SP600125 compared with VCA-treated cells (M1 83.03% in VCA-treated cells vs. 60.65% in SP600125-pretreated Hep3B cells) (Fig. 8D). In contrast, loss of $\Delta\Psi m$ induced by VCA was also significantly inhibited by SP600125 treatment (M1 84.04% in VCA-treated cells vs. 64.31% in JNK inhibitor-pretreated Hep3B cells), indicating that JNK activation play an important role in ROS production, loss of $\Delta\Psi m$, and apoptosis induced by VCA. However, this was not unexpected because JNK is generally a well described downstream target of ROS (Xia et al., 1995). Therefore, to define whether JNK is an upstream or downstream regulator of ROS production, we pretreated Hep3B cells with NAC, followed by treatment with VCA. In these experiments, JNK/SAPK phosphorylation and GST-c-jun kinase activity induced by VCA were unaffected with pretreatment of NAC (Fig. 8E), suggesting that JNK/SAPK

Molecular Pharmacology Fast Forward. Published on August 31, 2004 as DOI: 10.1124/mol.104.001347
This article has not been copyedited and formatted. The final version may differ from this version.

plays a role as an upstream regulator of ROS production, resulting in apoptosis.

A critical role for JNK1 overexpression in apoptosis induced by VCA. To further confirm the essential role of JNK activation in cell death, ROS production, and loss of $\Delta\Psi m$ by VCA, Hep3B cells were stably transfected with JNK1 cDNA, followed by treatment with VCA. As shown in Fig. 9A, greater levels of JNK proteins were detected in 3 different JNK1-transfected clones compared to vector-transfected clones. GST-c-jun phosphorylation induced by VCA was significantly increased in JNK1-transfected Hep3B cells, and remained strong after 60 min (Fig 9B). Next, we compared VCA-induced apoptosis in vector- and JNK1-transfected Hep3B cells by measuring DNA fragmentation and MTT assay. As shown in Fig. 9C, treatment with VCA induced significantly more apoptosis in JNK1-transfected Hep3B cells than in vector-transfected cells, which was also confirmed by FACS analysis (M1, sub-G1, $20.4 \pm 0.5\%$ in VCA-treated vector-transfected cells vs. $38.9 \pm 0.5\%$ in VCA-treated JNK1-transfected cells) (Fig. 9D).

Hep3B cells were stably transfected with dominant-negative JNK1 cDNA, followed by treatment with VCA. As shown in Fig. 10A-C, stable transfection of dominant-negative JNK1 abolished VCA-induced apoptosis. We then attempted to confirm the critical role of JNK1 in the potentiation of ROS production and loss of $\Delta\Psi m$. As expected, VCA-induced ROS production was significantly increased in wild type JNK1-transfected Hep3B cells (M1 73.03% in VCA-treated control cells vs. 89.05% in JNK1 overexpressing Hep3B cells), whereas ROS production was decreased in dominant-negative JNK-transfected cells (M1 58.95% in dominant negative JNK1 overexpressing Hep3B cells) (Fig. 10D left panel). Similar to effects observed with ROS production, the

Molecular Pharmacology Fast Forward. Published on August 31, 2004 as DOI: 10.1124/mol.104.001347
This article has not been copyedited and formatted. The final version may differ from this version.

loss of ΔΨm induced by VCA was also significantly increased in wild type JNK1-transfected Hep3B cells (M1 74.78% in VCA-treated control cells vs. 89.04% in JNK overexpressing Hep3B cells), whereas loss of ΔΨm was decreased in dominant-negative JNK1-transfected cells (M1 64.04% in dominant negative JNK overexpressing Hep3B cells) (Fig. 10D right panel). Combining these results, Hep3B cells transfected with wild type JNK1 are more susceptible to VCA-induced apoptosis, ROS production, and loss of ΔΨm, suggesting that JNK activation play an important role in these events.

The critical role of SEK, an upstream signal mediator of JNK, in ROS production and loss of ΔΨM **induced by VCA.** To examine the possible involvement of signal mediators upstream of JNK activation, Hep3B cells were stably transfected with wild type SEK or dominant-negative SEK cDNA. As shown in Fig. 11A, JNK phosphorylation by VCA significantly increased in wild type SEK1-transfected Hep3B cells compared with vector- and dominant negative SEK1-transfected cells. Next, to examine the functional role of JNK activation on apoptosis induced by VCA, we co-transfected pEGFP and wild type SEK1 or dominant-negative SEK1, and then performed the TUNEL assay and Hoechst 33258 staining. As shown in Fig. 11B and C, apoptosis induced by VCA was increased in GFP positive SEK1-transfected cells, observed as green fluorescence, but lower levels of apoptotic cells were detected in dominant-negative SEK1-transfected cells relative to vector-transfected cells, suggesting that VCA induces apoptosis through the SEK1-JNK1 signaling pathway in Hep3B cells. Measuring fluorescence intensity, VCA-induced ROS production and loss of ΔΨm in both vector- and wild type SEK1 or dominant-negative SEK1-transfected Hep3B cells were compared.

Molecular Pharmacology Fast Forward. Published on August 31, 2004 as DOI: 10.1124/mol.104.001347
This article has not been copyedited and formatted. The final version may differ from this version.

As shown in Fig. 11D, increased ROS production by VCA in wild type SEK1-transfected Hep3B cells was strongly abolished in dominant-negative SEK1-transfected cells (M1, 84.32±0.4 vs. 62.55±0.4). Also, the loss of $\Delta\Psi m$ induced by VCA in SEK1-transfected cells was abolished in dominant-negative SEK1-transfected cells (91.3 ± 0.5 vs. 69.47 ± 0.5). These results suggest that SEK1-JNK1 signaling pathway plays an essential role in ROS production, loss of $\Delta\Psi m$, and apoptosis induced by VCA.

Molecular Pharmacology Fast Forward. Published on August 31, 2004 as DOI: 10.1124/mol.104.001347
This article has not been copyedited and formatted. The final version may differ from this version.

Discussion

Numerous studies have demonstrated that VCA is a potent inducer of apoptosis in several cell lines, but the underlying mechanisms are not clear. In this study, we determined that VCA induces ROS production and loss of $\Delta\Psi m$ following the release of cytochrome C into the cytosol, and alters the ratio of Bax/Bcl-2 expression and Bax distribution. Furthermore, the SEK1-JNK1 signaling pathway may play an important role in the production of ROS, loss of $\Delta\Psi m$, and apoptosis induced by VCA in Hep3B cells.

During apoptosis, the protooncogene Bcl-2 is thought to control mitochondrial permeability transition, allowing for the release of cytochrome C (Esposti et al., 1999). The balance between the expression of anti- and proapoptotic proteins is important for controlling cell death in several cell types (Gross et al., 1999). Our data show that VCA enhances proapoptotic Bax protein expression, but decreases levels of the antiapoptotic proteins Bcl-2 and Bcl-xL when compared with control cells. In addition, cytochrome C release from the mitochondria into the cytosol was detected in VCA-treated cells, but considerable change in the expression of Bad, and Apaf-1 by VCA was undetected (Fig.3). Blocking caspase-3 activation with a specific inhibitor, z-DEVD-CHO, abolished VCA-induced apoptosis in Hep3B cells (Fig.2), which is consistent with our previous conclusion that VCA-induced apoptosis is caspase-3-dependent in the human leukemia cell line, HL-60 (Lyu et al., 2001), but had little effect on the change of Bcl-2-related proteins by VCA.

The activation of the proapoptotic molecule Bax are required to mediate cytochrome C release from mitochondria and regulate intrinsic apoptosis pathway involving the

mitochondria. In viable cell, a substantial portion of Bax is monomeric and found either in the cytosol or loosely attached to membranes. Following a death stimulus, cytosolic and monomeric Bax translocates to mitochondria where it becomes an integral membrane protein and cross-linkable as a homodimer, that results in release of cytochrome C (Putcha et al., 1999). Consistent with those reports, we also observed, after treatment of VCA, an increased Bax translocation from cytoplasm into outer mitochondrial membrane where it is thought to play a role in the release of proapoptotic factors, including cytochrome C, supporting our immunocytochemistry data using FITC-Bax and MitoTracker –CMXRos C (Fig.4A-B). Moreover, our data shows that VCA induces the oligomerization of Bax in a time-dependent manner, which is consistent with Bax translocation into mitochondria (Fig.4D). It has been also suggested that oligomerized Bax interacts with resident mitochondria protein such as VDAC, and affect the release of proapototic activator including cytochrome C (Wei et al., 2001). As shown in Fig,4C, the interaction of Bax with VDAC was significantly increased in VCA-treated cells consistent with previous reports. Collecting the data suggests that VCA-induced Bax conformational change could be an early event followed by cytochrome C release, caspase-3 activation and then apoptosis.

Mitochondrial damage is important in cell death, and in some models of apoptosis, damage may be an early event in apoptosis (Crompton, 1999) and is consistent with intracellular ROS production and changes in $\Delta\Psi m$ during apoptosis (Lemasters, 1999). Several studies have suggested that increased ROS production, preceding the loss of $\Delta\Psi m$, is correlated with the release of cytochrome C and caspase-3 activation in various

cell types (Esposti et al., 1999). However, it is unclear whether the increase in ROS levels following exposure to VCA is due to losses in ΔΨm and correlates with the release of cytochrome C and caspase-3 activation in our cell systems. Our study does show clear evidence, however, that VCA treatment significantly induces ROS production and loss of ΔΨm, which are both shown to occur prior to cell death (Fig.5A), and consistent with an alteration in Bax/Bcl-2 protein ratio, cytochrome C release, and activation of caspase-3 in Hep3B cells. Our results also show that oxidative stress plays a critical role in the regulation of ROS production and loss of ΔΨm induced by VCA, since antioxidants such as NAC and cyclosporine A (not shown) effectively prevented ROS production, loss of ΔΨm, and cell death(Fig.5). However, other antioxidants such as superoxide dismutase, deferoxamine, and catalase failed to rescue Hep3B cells from VCA-induced apoptosis (not shown). In contrast to our results, Lavastre et al. recently reported that VAA-1 alters mitochondrial transmembrane potential and increases intracellular levels of ROS in human neutrophils through ROS-independent and Mcl-1-dependent mechanisms. The reasons for the apparent in cellular responses after treatment with mistletoe lectins are unknown at this time. This apparent discrepancy may be due to the difference in the cell types, experimental conditions, and methods of lectin extraction used.

Currently, the underlying mechanism by which VCA induces ROS production and loss of ΔΨm in Hep3B cells is undefined. Several mitochondrial proteins including Bcl-2 and Bax may possible to play important roles in VCA-induced ROS and loss of ΔΨm, so the roles of these mitochondrial proteins in VCA-induced ROS production and loss of ΔΨm are further studying. The functions of the MAPKs are rather difficult to elucidate, but

some acceptable differences have been delineated. For instance, ERK is believed to preferentially regulate cell growth and differentiation (Minden and Karin, 1997), and the JNK and p38 MAPK function mainly in stress responses (Kyriakis et al., 1994). However, JNK and p38 MAPK can also be activated by mitogenic factors, such as epidermal growth factor, phorbol esters (Davis, 1993), and by T-cell activation (Brint et al., 2002). Thus, JNK and p38 seem to act not only in apoptosis, but also in mitogenic signaling. Recently, while ROS has been reported to activate ERK, JNK, and/or p38 MAPK signaling cascades (Yoshizumi et al., 2000), the role of these kinases in ROS signaling remains obscure. In particular, the direct relationship between MAPK activation and ROS production induced by VCA has not been extensively studied, although it was reported that cytotoxic lectin-II isolated from Korean mistletoe induced apoptotic cell death in the human leukemic cell line, U-937, via activation of ERK1/2, p38 MAPK, and JNK/SAPK (Park et al., 2000; Pae et al., 2001). In the present study, VCA strongly activates JNK/SAPK, but weakly activates ERK1/2 and p38 MAPK in Hep3B cells (Fig.7). Additionally, VCA-induced DNA fragmentation is not significantly enhanced when ERK1/2 and p38 MAPK activation is selectively inhibited by PD098059, an ERK1/2-specific inhibitor, and SB203580, a p38-specific inhibitor (not shown). Furthermore, we obtained similar results at lower concentrations of SP600125 (10 or 20 uM), since SP600125 is not a specific inhibitor of JNK/SAPK, but a broad MAPK inhibitor, especially, at the 30 uM concentration used in this experiments. From these results, we suggest that ERK1/2 and p38 MAPK do not have opposite effects on cell survival in cytotoxic responses by VCA, which may not contribute to the modulation of VCA-

Molecular Pharmacology Fast Forward. Published on August 31, 2004 as DOI: 10.1124/mol.104.001347
This article has not been copyedited and formatted. The final version may differ from this version.

mediated cytotoxic activity. Therefore, we studied the possibility that JNK/SAPK activation is involved in regulating ROS production, loss of ΔΨm, and apoptosis induced by VCA. Our data show that VCA synergistically enhances induction of ROS production, loss of ΔΨm, and apoptosis in wild type JNK1- (Fig.9) or SEK1-transfected cells (Fig.11), but weakly in SP600125-treated (Fig.8) cells and in dominant negative JNK1- or SEK1-transfected cells (Fig.10 and 11). These results show that JNK/SAPK activation may mediate ROS production and ΔΨm loss during apoptosis induced by VCA in Hep3B cells. However, it is difficult presently to directly link the ability of VCA to induce apoptosis solely through JNK activation in these cells, because the specific JNK inhibitor did not completely inhibit VCA-induced apoptosis. Further, our data show that VCA-induced apoptosis, ROS production, and loss of ΔΨm are only partially inhibited by blocking JNK activation by dominant-negative JNK1 or SEK1 transfection. This was not unexpected because JNK has been a well described downstream target of ROS (Yoshizumi et al., 2000; Xia et al., 1995). To define whether JNK is an upstream or downstream regulator of ROS production, we pretreated Hep3B cells with NAC, followed by treatment with VCA. Figure 8E show that JNK/SAPK phosphorylation and GST-c-jun kinase activity induced by VCA were unchanged with pretreatment of NAC, suggesting that JNK/SAPK is an upstream regulator of ROS production during apoptosis. However, we can hypothesize that VCA-induced ROS production and loss of ΔΨm are partially mediated through JNK activation since the possibility of other mechanisms involved in ROS production, loss of ΔΨm, and apoptosis induced by VCA have not been ruled out.

Recently, several studies have demonstrated that ROS production and apoptosis can be regulated through inhibition of NF-kB activation, and inactivation of the cell death effectors, caspase-3, 8, and -9 (Kowastoski et al., 1998). It is conceivable, although unproven in the present study, that VCA also activates T cells, and cell death may be mediated by several cytokines such as TNF-α or IFN-γ, which are produced by T cell activation. Studies regarding these potential candidate pathways are currently under investigation.

Finally, we conclude that VCA elicits apoptosis through ROS production and loss of ΔΨm partially mediated by JNK activation, followed by alteration of the Bax/Bcl-2 protein ratio, Bax translocation, cytochrome C release, and caspase-3 activation in Hep3B cells. Targeting this signaling pathway may offer therapeutic approaches in anticancer therapy in human hepatic cancers.

Molecular Pharmacology Fast Forward. Published on August 31, 2004 as DOI: 10.1124/mol.104.001347
This article has not been copyedited and formatted. The final version may differ from this version.

Acknowledgments

We thank Dr. BJ Song and MA Bae for providing JNK and SEK cDNA. We also thank Dr. Van-Anh Nguyen for peer reviewing this paper.

This work was supported by research grants from the Korean National Institutes of Health intramural research grant (347-6111-211-207).

REFERENCES

Allen, R. T., Cluck, M. W., Agrawal, D. K. (1998) Mechanisms controlling cellular suicide: role of Bcl-2 and caspases. Cell Mol Life Sci., 54:427-445.

Bai, J., Rodriguez, A. M., Melendez, J. A., Cederbaum, A. I. (1999) Overexpression of catalase in cytosolic or mitochondrial compartment protects HepG2 cells against oxidative injury. J Biol Chem., 274(37):26217-24.

Bantel, H., Engels, I. H., Voelter, W., Schulze-Ostheff, K., and Wesslborg, S. (1999) Mistletoe lectin activates caspase-8/FLICE independently of death receptor signaling and enhances anticancer drug-induced apoptosis. Cancer Res., 59: 2083-2090.

Bloksman, N., Dijk, H. V., Korst, P., Willer, J. M. (1979) Cellular and humoral adjuvant activity of mistletoe extract. Immunobiology, 156:309–19.

Brint, E.K., Fitzgerald, K. A., Smith, P., Coyle, A. J., Gutierrez-Ramos, J. C., Fallon, P.G., and O'Neill, L. A. (2002) Characterization of signaling pathways activated by the interleukin 1 (IL-1) receptor homologue T1/ST2. A role for Jun N-terminal kinase in IL-4 induction. J Biol Chem., 277(51):49205-11.

Büssing, A., Suzar, K., Bergmann, J., Pfüller, U., Schietzel, M., Schweizer, K. (1996) Induction of apoptosis in human lymphocytes treated with *Viscum album* L. is mediated by the mistletoe lectins. Cancer Lett., 99:59.

Büssing, A., Vervecken, W., Wagner, M., Wagner, B., Pfuller, U., Schietzel, M. (1999) Expression of mitochondrial Apo2.7 molecules and caspase-3 activation in human lymphocytes treated with the ribosome-inhibiting mistletoe lectins and the cell membrane permeabilizing viscotoxins. Cytometry, 37:133± 139

Crompton, M. (1999) The mitochondrial permeability transition pore and its role in cell death.Biochem J., 341:233-249.

Davis, R.J. (1993) The mitogen-activated protein kinase signal transduction pathway. *J Biol Chem*., 268:14553–14556.

Dietrich, J. B., Ribe´reau-Gayon, G., Jung, M. L., H., Franz, Beck, J. P., and Anton, R. (1992) Identity of the N-terminal sequences of the three A chains of mistletoe (*Viscum album* L.) lectins: homology with ricin-like plant toxins and single-chain ribosome-inhibiting proteins. *Anticancer Drugs, 3:50*.

Esposti, M. D., Hatzinisiriou, I., McLennan, H., Ralph, S. (1999) Bcl-2 and mitochondrial oxygen radicals. New approaches with reactive oxygen. J. Biol. Chem., 274:29831-29837.

Franz, H. (1986) Mistletoe lectins and their A and B chains. *Oncology,* 43: 23-34.

Gilmore, A. P., Metcalfe, A. D., Romer, L. H., and Streuli, C. H. (2000) Integrin-mediated survival signals regulate the apoptotic function of Bax through its conformation and subcellular localization. J. Cell Biol. 149: 431-446

Gross, A., McDonnell, J. M., Korsmeyer, S. J. (1999) BCL-2 family members and the mitochondria in apoptosis. Genes Dev.,13:1899-1911.

Gupta, S., Campbell, D., Derijard, B., and Davis, R. J. (1995) Transcription factor ATF2 regulation by the JNK signal transduction pathway. *Science,* **267:** 389–393.

Hajto, T., Hostanski, K., Fischer, J., Saller, R. (1998) Immunomodulatory effect of *Viscum album* agglutinin-I on natural immunity. Anti-Cancer Drugs,1:s43–6.

Hajto, T., Hostanska, K., Weber, K., Zinke, H., Fischer, J., Mengs, U., Lentzen, H., and

Saller, R. (1998) Effect of a recombinant lectin: *Viscum album* agglutinin on the secretion of interleukin-12 in cultured human peripheral blood mononuclear cells and on NK-cell-mediated cytotoxicity of rat splenocytes in vitro and in vivo. *Nat. Immun., 16:34*.

Khwaja, T. A., Varven, J. C., Pentecost, S., Pande, H. (1980) Isolation of biologically active alkaloids from Korean mistletoe Viscum album, coloratum. Experientia, 36:599-600.

Kowaltowski, A J., Netto, L. E., Vercesi, A. E. (1998) The thiol-specific antioxidant enzyme prevents mitochondrial permeability transition. Evidence for the participation of reactive oxygen species in this mechanism. J Biol Chem, 273:12766-12769.

Kyriakis, J. M., Banerjee, P., Nikolakaki, E., Dai, T., Rubie, E. A., Ahmad, M. F., Avruch, J., and Woodgett, J. R. (1994) The stress-activated protein kinase subfamily of c-Jun kinases. *Nature,* **369:** 156–160.

Lavastre, V., Pelleier, M., Saller, R., Hostanka, K., and Girard, D. (2002) Mechanisms involved in spontaneous and viscum album agglutinin-I-induced human neutrophil apoptosis: Viscum album agglutin-I accelerated the loss of antiapoptotic Mcl-1 expression and the degradation of cytoskeletal paxillin and vimentin proteins via caspases. J. of Immunology, 168:1419-1427.

Leist, M., Single, B., Castoldi, A. F., Kuhnle, S., & Nicotera, P. (1997) Intracellular adenosine triphosphate (ATP) concentration: a switch in the decision between apoptosis and necrosis. *J Exp Med., 185* : 1481–1486.

Lemasters, J. J. (1999) Necrapoptosis and the mitochondrial permeability transition: shared pathways to necrosis and apoptosis. Am J Physiol., 276: G1-G6.

Lyu, S. Y., Park, W. B., Choi, K. H., Kim, W. H. (2001) Involvement of caspase-3 in apoptosis induced by Viscum album var. coloratum agglutinin in HL-60 cells. *Biosci Biotechnol Biochem.* 65:534.

Lyu, S. Y., Choi, S. H., Park, W. B. (2002) Korean mistletoe lectin-induced apoptosis in hepatocarcinoma cells is associated with inhibition of telomerase via mitochondrial controlled pathway independent of p53. Arch Pharm Res., 25(1):93-101.

Majewski N., Nogueira V., Brooks Robey R., and Hay N. (2004) Akt inhibits apoptosis downstream of bid cleavage via a glucose-dependent mechanism involving mitochondrial hexokinases. Mol. Cell Bio. 24: 730-740.

Minden, A., and Karin, M. (1997) Regulation and function of the JNK subgroup of MAPKinases. Biochim. Biophys. Acta., 1333:F85-F104.

Na, S., Chung, H. T., Cunningham, A., Turi, T. G., Hanke, J. H., Bokoch, G. M., and Danley, D. E. (1996) D4-GD1, a substrate of CPP32, is proteolyzed during Fas-induced apoptosis. J. Biol. Chem. 271:11209-11213.

Pae, H. O., Oh, G. S., Kim, N. Y., Shin, M. K., Lee, H. S., Yun, Y.G., Oh, H., Kim, Y. M., and Chung, H. T. (2001) Roles of extracellular signal-regulated kinase and p38 mitogen-activated protein kinase in apoptosis of human monoblastic leukemia U937 cells by lectin-II isolated from Korean mistletoe. In Vitr Mol Toxicol., 14 (2): 99-106.

Park, R.K., Kim, M.S., So, H.S., Jung, B.H., Moon, S.R., Chung, S.Y., Ko, C.B., and Chung, H.T. (2000) Activation of c-Jun N-terminal kinase1 (JNK1) in mistletoe lectin-II-induced apoptosis of human myeloleukemic U937 cells. Biochem. Pharmacol., 60:1685-1691.

Park, W.B., Ju, Y., and Han, S. K. (1998) Isolation and characterization of –galactoside specific lectin from korean mistletoe with lactose-BSA-sepharose 4B and changes of lectin conformation. Arch. Pharm. Res., 21: 429-535.

Park, W. B., Lyu, S.Y., Kim, J. H., Choi, S. H., Chung, H. K., Ahn, S. H., Hong, S.Y., Yoon, T. J., Choi, M. J. (2001) Inhibition of tumor growth and metastasis by Korean mistletoe lectin is associated with apoptosis and antiangiogenesis. Cancer Biother Radiopharm., 16(5):439-47.

Pastorino, J. G., & Hoek, J. B. (2001) Ethanol potentiates tumor necrosis factor-_ cytotoxicity in hepatoma cells and primary rat hepatocytes by promoting induction of the mitochondrial permeability transition. *Hepatology, 31:* 1141–1152.

Putcha, G. V., Deshmukh, M., and Johnson, E. M., Jr. (1999) BAX translocation is a critical event in neuronal apoptosis: regulation by neuroprotectants, BCL-2, and caspases. J. Neurosci. 19: 7476-7485

Savoie, A., Lavastre, V., Pelletier, M., Hajto, T., Hostanska, K., and Girard. D. (2000) Activation of human neutrophils by the plant lectin *Viscum album* agglutinin-I: modulation of de novo protein synthesis and evidence that caspases are involved in induction of apoptosis. *J. Leukocyte Biol., 68:845*.

Soh Y., Jeong K. S., Lee I., Bae M. A., Kim YC., and Song B. J. (2000) Selective activation of the c-jun N-terminal Protein Kinase pathway during 4-Hydroxynonenal-induced apoptosis of PC12 cells. Mol. Pharmacol. 58: 535-541

Wei, M. C., Zong, W. X., Cheng, E. H., Lindsten, T., Panoutsakopoulou, V., Ross, A. J., Roth, K. A., macGregor, G. R., Thompson, C. B., and Korsmeyer, S. J. (2001)

Proapoptotic BAX and BAK: a requisite gateway to mitochondrial dysfunction and death. Science 292: 727-730.

Xia, Z., Dickens, M., Raingeaus, J., Davis, R. J., and Greenberg, M. E. (1995) Opposing effects of ERK and JNK-p38 MAP kinases on apoptosis. Science (Wash DC), 270:1326-1331.

Yoon, T. J., Yoo, Y. C., Choi, O. B., Do, M. S., Kang, T. B., Lee, S.W., Azuma, I., Kim, J. B. (1995) Inhibitory effect of Korean mistletoe (Viscum album coloratum) extract on tumour angiogenesis and metastasis of haematogenous and nonhaematogenous tumour cells in mice. *Cancer Lett*, 97:83-91.

Yoshizumi, M., Abe, J., Haendeler, J., Huang, Q., Berk, B. C. (2000) Src and cas mediate JNK activation but not ERK1/2 and p38 kinases by reactive oxygen species. *J Biol Chem*., 275:11706–11712.

Footnotes

This work was supported by research grants from the Korean National Institutes of Health for the 2003 program year.

To receive Reprint requests: Dr. Myeong Ho Jung, Division of Metabolic Disease, Department of Biomedical Science, National Institutes of Health, #5 Nokbun-dong, Eunpyung-gu, Seoul 122-701, South Korea. Tel: +82-2-380-1530; Fax: +82-2-354-1057; Email: jung0603@nih.go.kr

Molecular Pharmacology Fast Forward. Published on August 31, 2004 as DOI: 10.1124/mol.104.001347
This article has not been copyedited and formatted. The final version may differ from this version.

Figure legends

Fig. 1. The effects of VCA on apoptosis in Hep3B cells. Hep3B cells were treated with different concentrations of VCA for the indicated time points. (A) Cell viability was determined by the MTT assay. (B) Cellular DNA fragmentation was analyzed by agarose gel electrophoresis. (C) Morphology of untreated or VCA-treated Hep3B cells for 12h was visualized by Hoechst 33258 staining (x 200). Arrows indicate apoptotic cells showing apoptotic bodies, nuclear cleavage, and chromatin condensation. (D) TUNEL assay was carried out and pictures were taken under a fluorescent microscope. Arrows indicate the apoptotic cells. (E) Apoptotic cells were quantified by flow cytometry. Apoptosis (M1, sub-G1 peak) was measured by PI staining. (A and E) Results represent the average ±S.E.M. from 3 to 5 independent experiments. (B)-(D) are representatives of 4 independent experiments. Similar results were obtained for each of the 4 experiments.

Fig. 2. The effects of caspase-3 activation on apoptosis induced by VCA in Hep3B cells. Hep3B cells were treated with 10 ng/mL VCA for various time points (A) and at different concentrations (B) in the absence or presence of the caspase-3 inhibitor, z-DEVD-CHO, and then caspase-3 activity was measured. Values shown are means ±S.E.M. from 3 independent experiments. Significant differences from untreated controls are indicated (∗$p < 0.05$, ∗∗$p < 0.01$) (C) Apoptosis was analyzed by DNA fragmentation. (D) Cell extracts were prepared and subjected to Western blotting using an anti-PARP antibody. The 86 kDa band represents the cleaved PARP. (C) and (D) are representative

of 3 independent experiments. Similar results were obtained for each of the 4 experiments.

Fig. 3. Immunoblot changes in expression of proapoptotic and antiapoptotic proteins by VCA in Hep3B cells. Cells were treated with VCA for the indicated time points. (A) Expression of Bax, Bcl-2, Bcl-xL, Bad, and Apaf-1 proteins in Hep3B cells. Whole cell lysates were separated on SDS-PAGE, followed by immunoblotting. Each target protein was detected with the specific antibody against Bax, Bcl-2, Bcl-xL, Bad, and Apaf-1. Re-probing was done with actin by immunoblotting as a loading control. (B) Cells were treated with VCA in the absence or presence of the caspase-3 inhibitor, z-DEVD-CHO, and then subjected to Western blotting. (C) Release of cytochrome C into the cytosol from Hep3B mitochondria. After incubation with VCA, mitochondrial and cytosolic fractions were separated and cytochrome C content was analyzed by Western blotting.

Fig. 4. VCA induces Bax translocation into mitochondria and induces Bax oligomerization. Cells were treated with VCA for the indicated time points. **(A)** Bax translocation into mitochondria by VCA. Fluorescent microscopic images taken for Bax, MitoTracker CMXRos, and the final merged images are shown. (B) Increased binding of Bax to the mitochondria-enriched fraction. After incubation with VCA, mitochondrial and cytosolic fractions were separated and analyzed by Western blotting for Bax and VDAC. (C) Mitochondria-enriched fraction was immunoprecipitated with anti-VDAC, and immunoprecipitates were analyzed by Western blotting using the specific antibody against anti-Bax. (D) VCA induces Bax oligomerization. The mitochondria-enriched

Molecular Pharmacology Fast Forward. Published on August 31, 2004 as DOI: 10.1124/mol.104.001347
This article has not been copyedited and formatted. The final version may differ from this version.

fraction was isolated at different times after VCA treatment. The isolated mitochondrial fractions were subjected to protein cross-linking with bismaleimidohexane. Following cross-linking, mitochondria were boiled and subjected to Western blot using anti-Bax antibody. All data are representative of 3 independent experiments. Similar results were obtained for each of the 3 experiments.

Fig. 5. The effects of VCA on production of ROS and ΔΨm in Hep3B cells. (A) Cells were incubated with VCA for 12 h in the absence or presence of NAC, and then harvested by trypsinization. After 30 min of incubation with DCFH-DA (5μM) for ROS (left panel) and DiOC6 (100nM) for ΔΨm (right panel), intracellular fluorescence intensity was measured by FACScan flow cytometry (M1, the percentage of ROS production and loss of ΔΨm). The numbers gated in the each phase areas are mean ±S.E.M of three experiments (B) Fluorescence intensity of DCF and DiOC6 in Hep3B cells were quantified and the percent change in ROS production and loss of ΔΨm was determined relative to control. Significant differences from untreated controls are indicated (∗P< 0.05, ∗∗P< 0.01). (C) Inhibition of VCA-induced apoptosis by NAC was determined by DNA fragmentation. (B)-(C) is representative of 4 independent experiments. Similar results were obtained for each of the 4 experiments.

Fig. 6. The changes of mitochondrial membrane transition by VCA in Hep3B cells. (A) Cells were incubated with tetramethylrhodamine methyl ester (TMRM) and observed using a laser scanning confocal microscope. Following the collection of a baseline image,

the cells were either treated with vehicle or VCA (10 ng/ml), and visualized at 5 min intervals for 2 h as described in "Materials and Methods." (B) Fluorescence intensity of TMRM in Hep3B cells was quantified. Significant differences from untreated controls are indicated (∗P< 0.01, ∗∗P<0.05). (C) Cells were treated with VCA in the absence or presence of the antioxidant inhibitor, NAC, and then subjected to Western blotting. Data are representative of 3 independent experiments. Similar results were obtained for each of the 3 experiments.

FIG. 7. The effects of VCA on MAPKs activation in Hep3B cells. The cells were treated with VCA for the indicated time points. (A) Whole-cell lysates prepared at different time points were subjected to SDS-PAGE followed by immunoblot analyses using the specific antibodies against α-phospho-JNK1, JNK1, phosphor-ERK1/2, ERK1/2, phosphor-p38, and p38. (B) Whole cell lysates were subjected to the JNK kinase assay using GST-c-jun as a substrate, and immunoprecipitates were analyzed by Western blotting using the specific antibody against anti-JNK. VCA-mediated phosphorylation and relative amounts of SEK1 in Hep3B cells were determined by immunoblot analysis using the specific antibody against phosphor-SEK1 and SEK1 protein. (A) and (B) are representative of 3 independent experiments. Similar results were obtained for each of the 3 experiments.

FIG. 8. The effects of JNK specific inhibitor, SP600125, on VCA-induced apoptosis, ROS production, and loss of ΔΨm in Hep3B cells. Cells were pretreated with 30 uM

SP600125 for 2h before exposure to VCA (10 ng/ml) for 12 h. (A) Whole cell lysates were subjected to JNK kinase assay using GST-c-jun as a substrate, and immunoprecipitates were analyzed by Western blotting using the specific antibody against anti-JNK. (B) Inhibition of VCA-induced apoptosis by SP600125 was determined by DNA fragmentation. (C) Apoptotic cells were analyzed by flow cytometry. The DNA content of each phase was quantified and the percent change is shown (Right panel). Significant differences from untreated controls are indicated ($*P< 0.05$, $**P< 0.01$). (D) After 30 min of incubation with DCFH-DA (5μM) for ROS (left panel) and DiOC6 (100nM) for $\Delta\Psi m$ (right panel), the intracellular fluorescence intensity was measured. (E) Cells were pretreated with 20 uM NAC for 2 h before exposure to VCA. Whole cell lysates were subjected to JNK kinase assay using GST-c-jun as a substrate, and immunoprecipitates were analyzed by Western blotting. JNK phosphorylation was analyzed using the specific antibody against anti-phospho-JNK antibody. All data are representative of 4 independent experiments. Similar results were obtained for each of the 4 experiments.

FIG. 9. The effects of wild type JNK1 (wt JNK1) overexpression on VCA-induced apoptosis in Hep3B cells. (A) Hep3B cells were stably transfected with either an empty vector or wild type JNK1 (wt JNK1) expression vector as described in "Materials and Methods." Three empty vector-transfected (Neo1, Neo2, Neo3) clones and 3 wild type JNK1-transfected clones (wt JNK1-1, wt JNK1-2, wt JNK1-3) were selected to be subjected to Western blot analysis using anti-JNK1 and β-actin antibodies. (B) A vector-

transfected (Neo1) and a wt JNK1-transfected clone (wt JNK1-2) were treated with VCA (10 ng/mL) for various time points, and the whole cell lysates were subjected to JNK kinase assay. (C) Cell viability was then measured by the MTT reduction method. Significant differences from untreated controls are indicated (∗P< 0.05, ∗∗P< 0.01). VCA-induced apoptosis in wild type JNK-transfected cells was also determined by DNA fragmentation (small box). (D) Apoptotic cells were analyzed by flow cytometry. All data are representative of 3 independent experiments. Similar results were obtained for each of the 3 experiments.

FIG. 10. The effects of dominant negative JNK1 (D/N JNK1) overexpression on VCA-induced apoptosis, ROS production, and loss of ΔΨm in Hep3B cells. (A) Hep3B cells stably transfected with dominant-negative JNK1 cDNA were treated with VCA as indicated. VCA-induced apoptosis in wild type JNK1-transfected cells was determined by DNA fragmentation. (B) A vector-transfected (Neo1) and a dominant-negative JNK1-transfected clone (D/N JNK1) were treated with VCA, followed by FACS analysis. (C) Cell viability was then measured by the MTT reduction method. Significant differences from untreated controls are indicated (∗P< 0.05, ∗∗P< 0.01). (D) The intracellular fluorescence intensity of DCF and DiOC6 was measured by FACScan flow cytometry. All data are representative of 4 independent experiments. Similar results were obtained for each of the 4 experiments.

FIG. 11. The effects of SEK1 overexpression on VCA-induced apoptosis, ROS

Molecular Pharmacology Fast Forward. Published on August 31, 2004 as DOI: 10.1124/mol.104.001347
This article has not been copyedited and formatted. The final version may differ from this version.

production, and loss of ΔΨm in Hep3B cells. (A) Hep3B cells stably transfected with wild type SEK1 (wt SEK1) and dominant-negative SEK1 cDNA were treated with VCA, and whole cell lysates were subjected to JNK kinase assay. (B) Hep3B cells were cotransfected with pEGFP and the expression vector encoding for wild type SEK1. After 36 h of transfection, the cells were treated with VCA for 12 h and fixed in 4% paraformaldehyde and analyzed by the TUNEL assay (Middle). GFP positive cells (Left) and cell morphology were visualized under a fluorescence microscope (x 200). The cells were also stained with Hoechst 33258 (Right). Arrows indicate the apoptotic cells. (C) Apoptotic cells induced by VCA in wild type SEK and dominant-negative SEK1-transfected Hep3B cells were quantified. GFP-positive cells were analyzed for the presence of apoptotic nuclei with a fluorescence microscope. The results shown are means ±S.E.M. from 3 independent experiments. Significant differences from untreated controls are indicated (∗P< 0.05, ∗∗P< 0.01). (D) The intracellular fluorescence intensity of DCF and DiOC6 was measured by FACScan flow cytometry. Data are representative of 4 independent experiments. Similar results were obtained for each of the 4 experiments.

Molecular Pharmacology Fast Forward. Published on August 31, 2004 as DOI: 10.1124/mol.104.001347
This article has not been copyedited and formatted. The final version may differ from this version.

Fig. 1

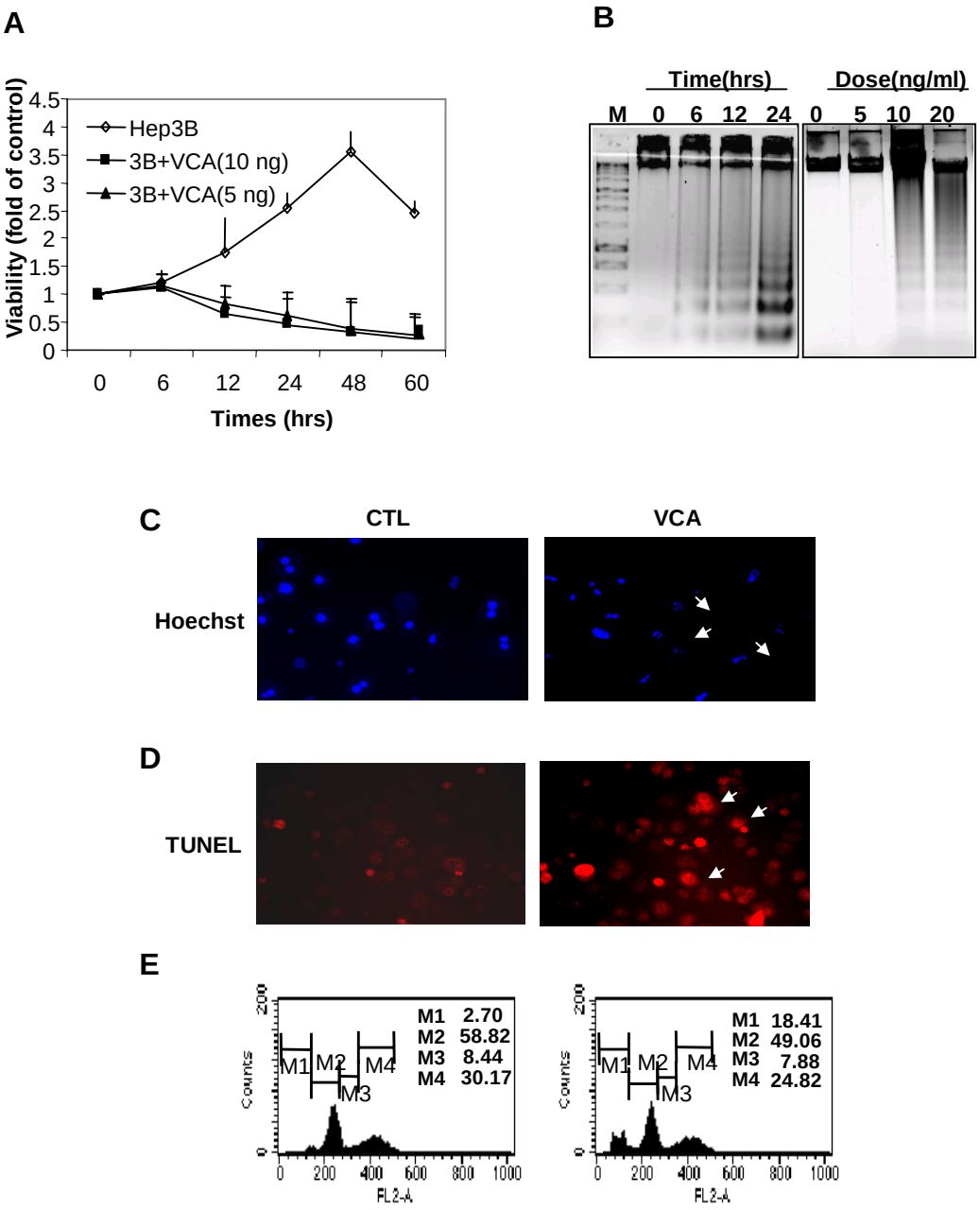

Molecular Pharmacology Fast Forward. Published on August 31, 2004 as DOI: 10.1124/mol.104.001347
This article has not been copyedited and formatted. The final version may differ from this version.

Fig. 2

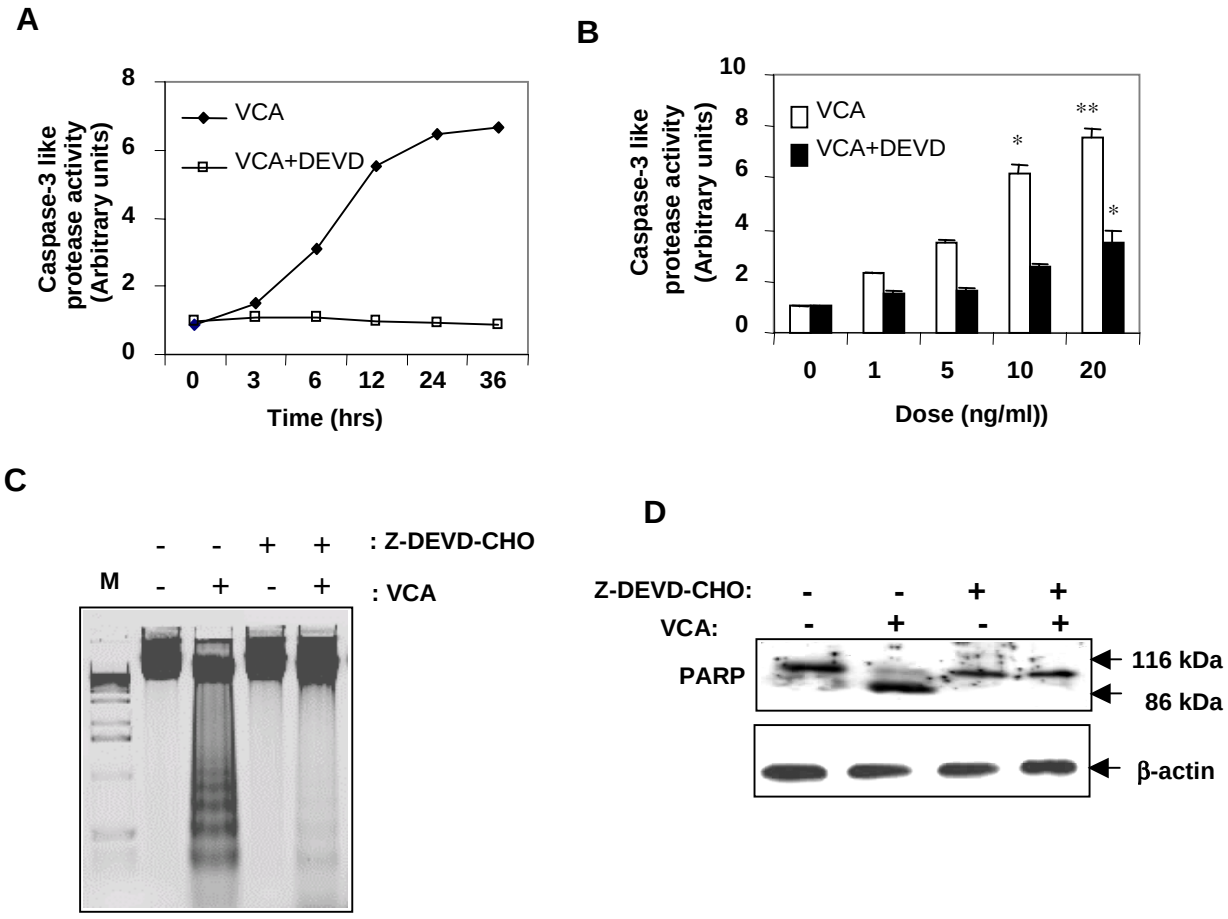

Molecular Pharmacology Fast Forward. Published on August 31, 2004 as DOI: 10.1124/mol.104.001347
This article has not been copyedited and formatted. The final version may differ from this version.

Fig. 3

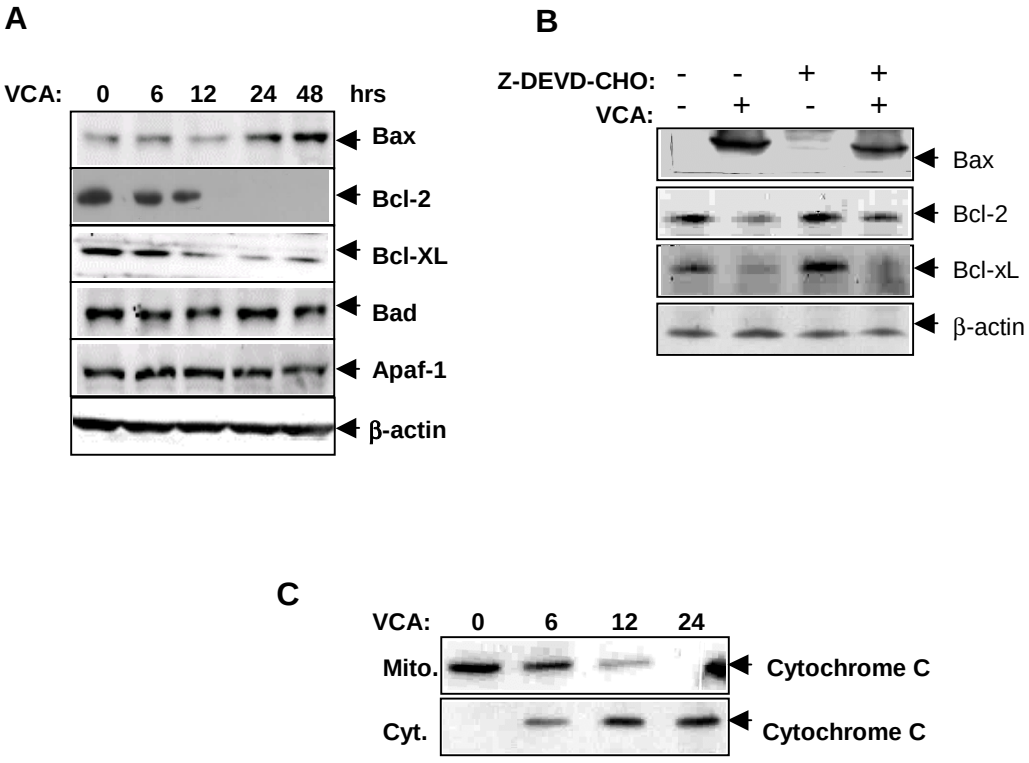

Molecular Pharmacology Fast Forward. Published on August 31, 2004 as DOI: 10.1124/mol.104.001347
This article has not been copyedited and formatted. The final version may differ from this version.

Fig. 4

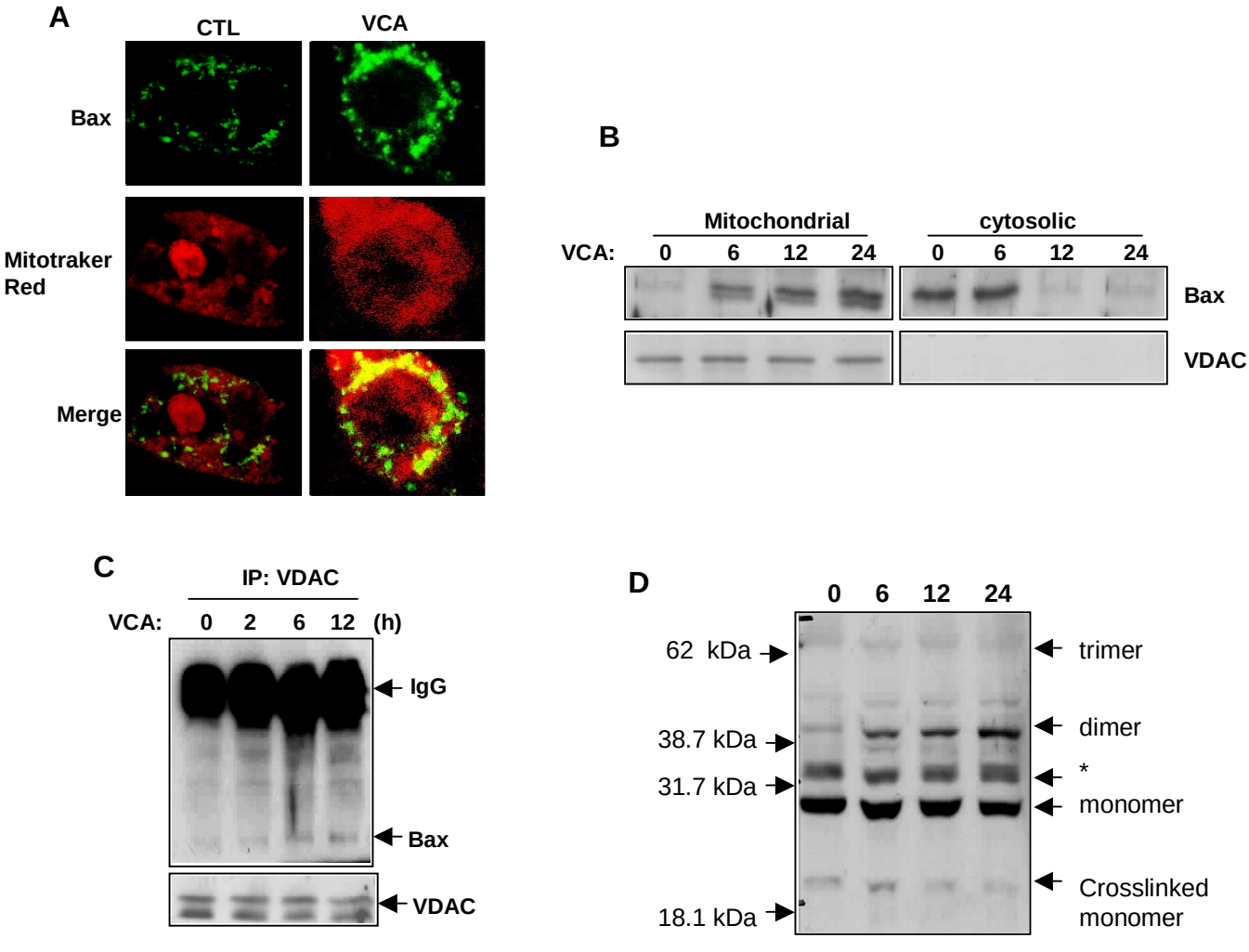

Molecular Pharmacology Fast Forward. Published on August 31, 2004 as DOI: 10.1124/mol.104.001347
This article has not been copyedited and formatted. The final version may differ from this version.

Fig. 5

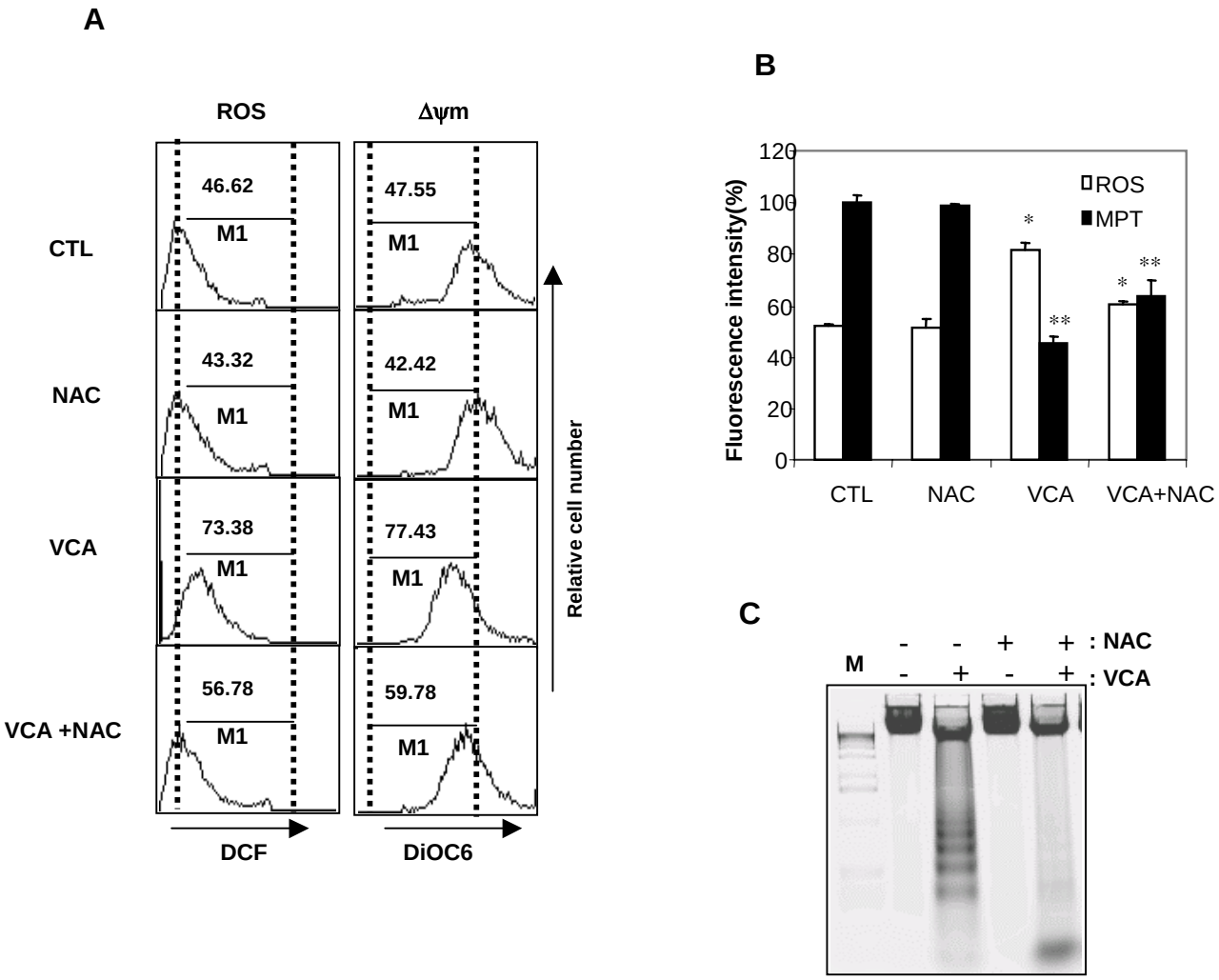

Molecular Pharmacology Fast Forward. Published on August 31, 2004 as DOI: 10.1124/mol.104.001347
This article has not been copyedited and formatted. The final version may differ from this version.

Fig. 6

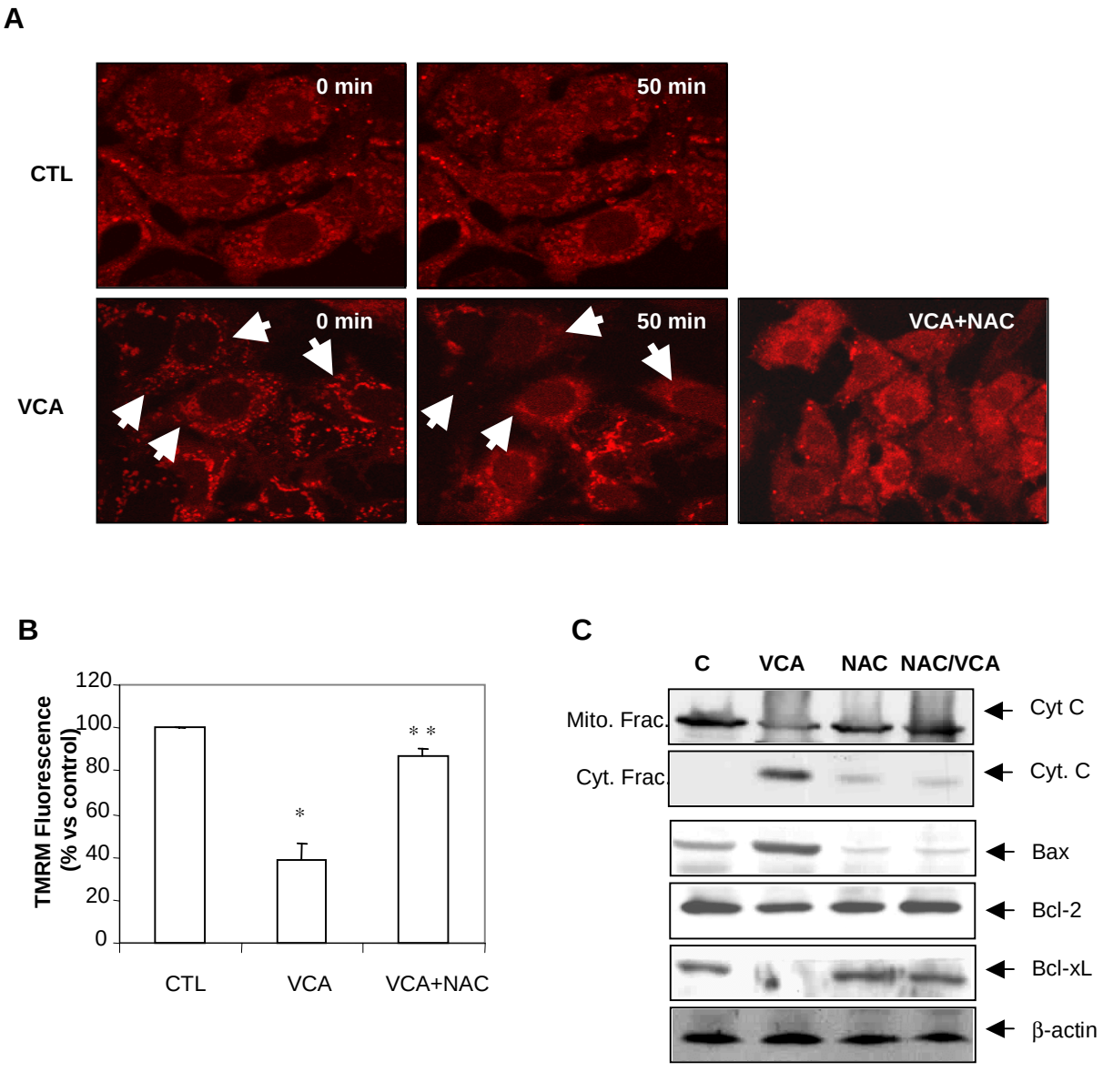

Molecular Pharmacology Fast Forward. Published on August 31, 2004 as DOI: 10.1124/mol.104.001347
This article has not been copyedited and formatted. The final version may differ from this version.

Fig. 7

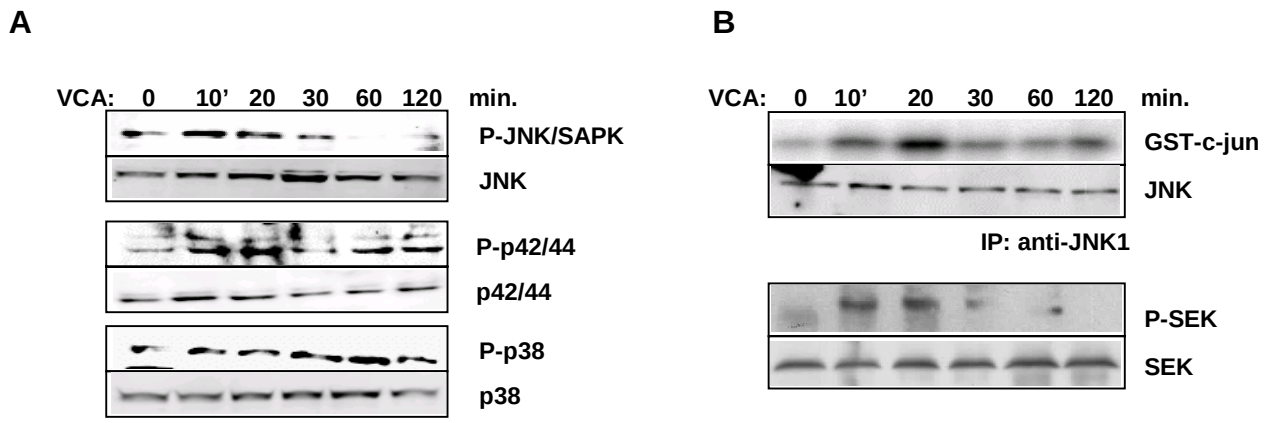

Molecular Pharmacology Fast Forward. Published on August 31, 2004 as DOI: 10.1124/mol.104.001347
This article has not been copyedited and formatted. The final version may differ from this version.

Fig. 8

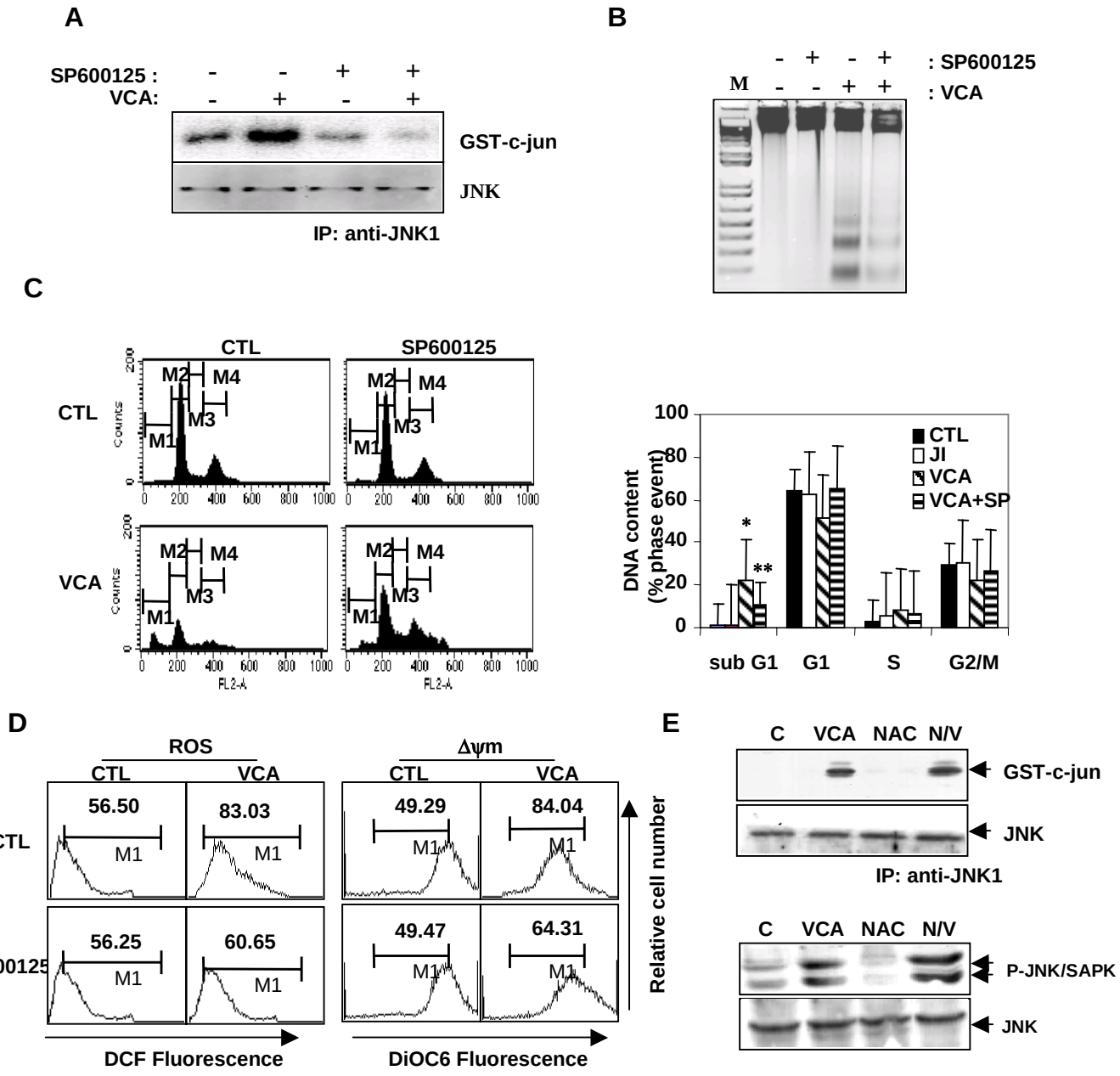

Molecular Pharmacology Fast Forward. Published on August 31, 2004 as DOI: 10.1124/mol.104.001347
This article has not been copyedited and formatted. The final version may differ from this version.

Fig. 9

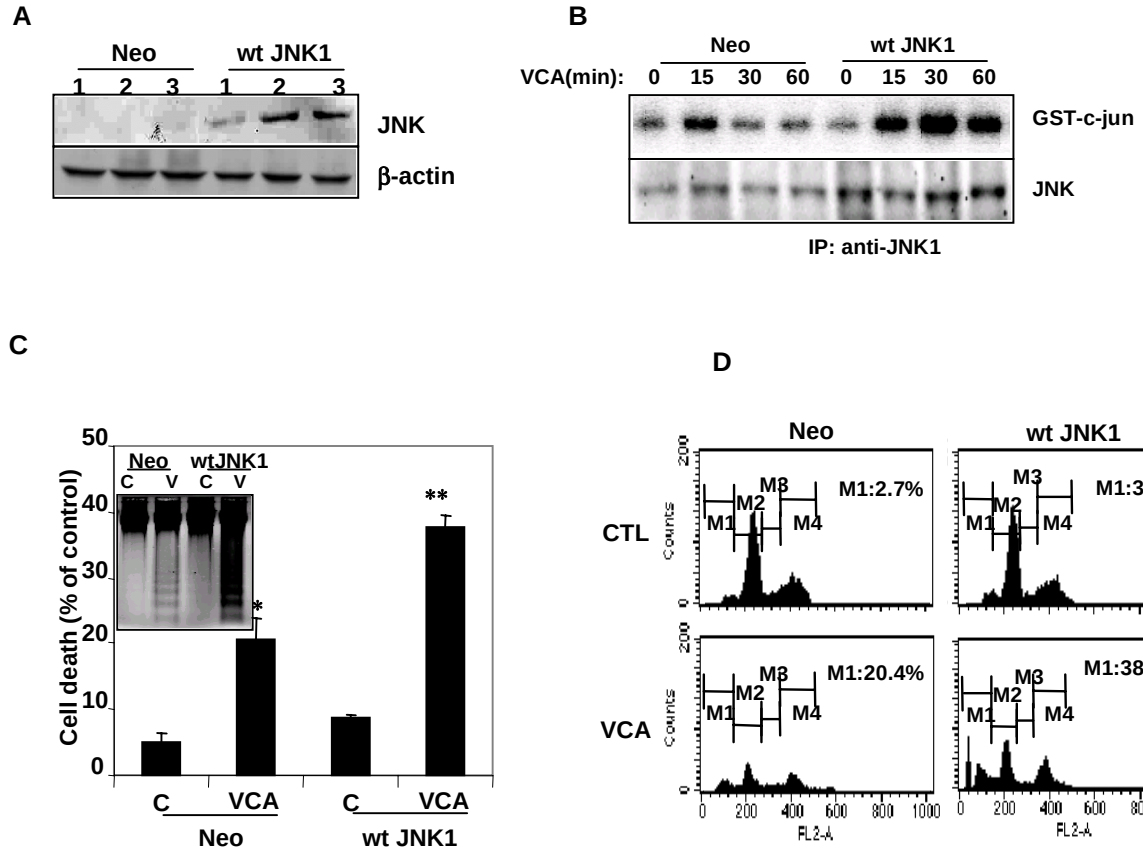

Molecular Pharmacology Fast Forward. Published on August 31, 2004 as DOI: 10.1124/mol.104.001347
This article has not been copyedited and formatted. The final version may differ from this version.

Fig. 10

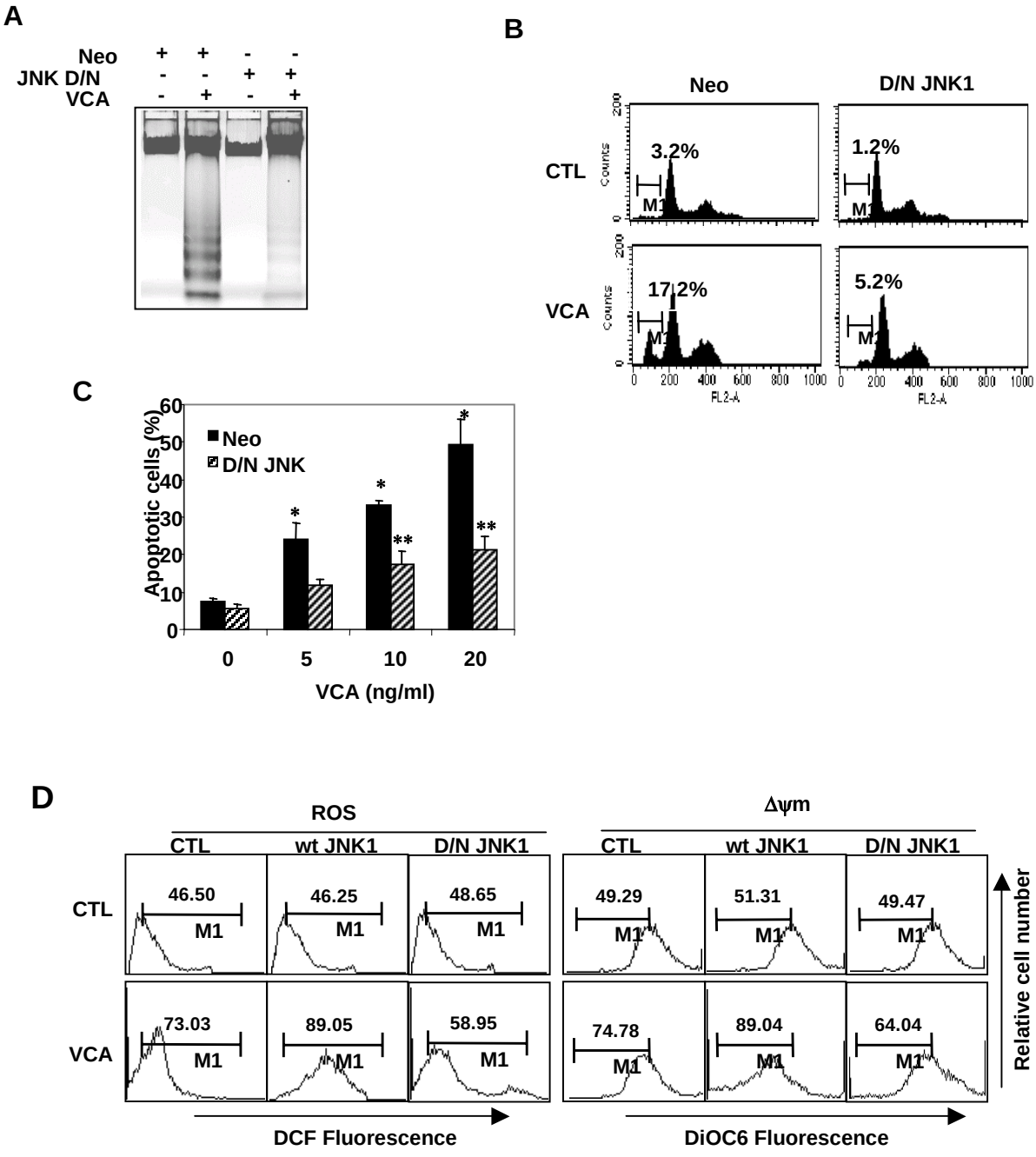

Molecular Pharmacology Fast Forward. Published on August 31, 2004 as DOI: 10.1124/mol.104.001347
This article has not been copyedited and formatted. The final version may differ from this version.

Fig. 11